

On the zeros of component functions of the Riemann Xi approximates

Surl-Hee (Shirley) Ahn

A THESIS

in

Mathematics

Presented to the Faculties of the University of Pennsylvania in Partial

Fulfillment of the Requirements for the Degree of Master of Arts

2012

Supervisor of Thesis

Graduate Group Chairman

Acknowledgments

First, I would like to thank my thesis adviser Jim Haglund, who made it possible for me to write a math master's thesis at Penn. Without his help and support, I would not have been able to have this invaluable experience of doing math research. I have immensely enjoyed working on my given topic for the thesis and I wish that I had more time to explore the topic further. It was wonderful seeing the empirical evidence that supported the Riemann Hypothesis and I would love to see more work being done in this field. I also sincerely hope to see a proof of the Riemann Hypothesis in my lifetime.

Second, I would like to acknowledge Jerry Kazdan, Michael Pimsner, and Sneha Subramanian, who were my mentors in the math department. Without their help and guidance, I would have not been able to pass the math preliminary exam and solidify my understanding of undergraduate mathematics. I would like to extend my gratitude to Ponzy Lu and Srilata Gangulee, who made it possible for me to pursue two master degree programs in chemistry and mathematics at Penn.

Lastly, I am grateful for family and friends who have supported me throughout my five years at Penn.

Abstract

It has been proven that the conjecture on the monotonicity of the zeros of the Riemann Xi approximates implies the Riemann Hypothesis. To explore this conjecture further, we computed and came up with conjectures on the zeros of the component functions of the Riemann Xi approximates. That is, we looked at the zeros of incomplete gamma functions, hyperbolic gamma functions, and linear combinations of Φ_n 's, which are functions that make up the Riemann Xi approximates. Specifically, we checked to see if there exist monotone zeros and interlacing between the zeros of the function and of its derivative.

Dedicated to my loving parents

Contents

1	The Riemann Hypothesis and the Riemann Xi function	1
2	Zeros of the Incomplete Gamma Function	11
3	Zeros of the Hyperbolic Gamma Function	15
4	Zeros of the Linear Combination of Φ_n 's	24
5	Appendix	30

1 The Riemann Hypothesis and the Riemann Xi function

One of the most famous unsolved problems in mathematics today is the Riemann Hypothesis. The German mathematician Georg Friedrich Bernhard Riemann (1826–1866) stated that all non-trivial zeros of the Riemann zeta function have $\operatorname{Re}(s) = \frac{1}{2}$.

To understand the hypothesis more clearly, we first looked at the Riemann zeta function. We initially defined the Riemann zeta function to be the Dirichlet series

$$\zeta(s) := 1 + \frac{1}{2^s} + \frac{1}{3^s} + \frac{1}{4^s} + \dots = \sum_{n=1}^{\infty} \frac{1}{n^s}, \quad (1.1)$$

where $s \in \mathbb{C}$ and $\operatorname{Re}(s) > 1$. Note that when $\operatorname{Re}(s) \leq 1$, the series (1.1) diverges and when $\operatorname{Re}(s) > 1$, the series (1.1) converges and defines an analytic function in this half-plane region.

To extend the Riemann zeta function to the $\operatorname{Re}(s) \leq 1$ region, we used analytic continuation. That is, suppose we are given a pair of functions f and F analytic in regions Ω and Ω' , respectively, with $\Omega \subset \Omega'$. If the two functions agree on the smaller set Ω , we say that F is an analytic continuation of f into the region Ω' [SS03]. The following theorem then guarantees that there can be only one such analytic continuation, since F is uniquely determined by f .

Theorem 1.1. *Suppose f and g are holomorphic in a region Ω and $f(z) = g(z)$ for*

all z in some non-empty open subset of Ω (or more generally for z in some sequence of distinct points with limit point in Ω). Then $f(z) = g(z)$ throughout Ω [SS03].

Riemann proved that $\zeta(s)$ can be continued analytically to an analytic function over the whole complex plane, except for the point $s = 1$, where $\zeta(s)$ has a simple pole with residue 1. Hence, we had the following definition for the Riemann zeta function $\zeta(s)$.

Definition 1.2. The Riemann zeta function $\zeta(s)$ is the analytic continuation of the Dirichlet series (1.1) to the whole complex plane, except for the point $s = 1$ [BCRW08].

After defining the Riemann zeta function, we looked at its properties, particularly the location of its zeros.

Theorem 1.3. *The Riemann zeta function $\zeta(s)$ satisfies the following:*

1. *The only zeros of $\zeta(s)$ outside the strip $0 \leq \operatorname{Re}(s) \leq 1$ are at the negative even integers, $-2, -4, -6, \dots$. We call these the trivial zeros [SS03].*
2. *$\zeta(s)$ has no zeros on the line $\operatorname{Re}(s) = 1$ [SS03].*
3. *The only pole of $\zeta(s)$ is at $s = 1$. The pole is simple with residue 1 [BCRW08].*
4. *The non-trivial zeros lie inside the region $0 \leq \operatorname{Re}(s) \leq 1$ and are symmetric about both the vertical line $\operatorname{Re}(s) = \frac{1}{2}$ and the real axis $\operatorname{Im}(s) = 0$ [BCRW08].*

Finally, Riemann stated his famous conjecture about the non-trivial zeros of the Riemann zeta function $\zeta(s)$.

Conjecture 1.4. (*The Riemann Hypothesis*) *All non-trivial zeros of the Riemann zeta function $\zeta(s)$ lie on the line $\text{Re}(s) = \frac{1}{2}$.*

After formally covering the Riemann Hypothesis, we looked at related functions that closely relate to the Riemann zeta function. Specifically, we looked at the Riemann xi function, a modification of the Riemann zeta function that Riemann introduced in his 1859 paper. For any $s \in \mathbb{C}$, the Riemann xi function is defined as

$$\xi(s) := \frac{s}{2}(s-1)\pi^{-\frac{s}{2}}\Gamma\left(\frac{s}{2}\right)\zeta(s). \quad (1.2)$$

This function is analytic everywhere in the complex plane and satisfies the following relation: $\xi(1-s) = \xi(s)$ for all $s \in \mathbb{C}$. In fact, the zeros of $\xi(s)$ are precisely the non-trivial zeros of $\zeta(s)$ [BCRW08]. Note that since $\xi(s)$ is a real-valued function when $\text{Re}(s) = \frac{1}{2}$, we can calculate the zeros of $\zeta(s)$ that lie on the line $\text{Re}(s) = \frac{1}{2}$ by determining where the function changes sign [BCRW08]. Hence, we looked at the Riemann Xi (uppercase xi) function, which is precisely

$$\Xi(t) \equiv \xi(s), \quad (1.3)$$

where $s \equiv \frac{1}{2} + it$ and $t \in \mathbb{R}$. This function can also be defined as

$$\Xi(it) \equiv \xi\left(\frac{1}{2} - t\right) = \xi\left(\frac{1}{2} + t\right) \quad (1.4)$$

$$= \frac{1}{2}\left(\frac{1}{2} + t\right)\left(-\frac{1}{2} + t\right)\pi^{-1/4-t/2}\Gamma\left(\frac{t}{2} + \frac{1}{4}\right)\zeta\left(t + \frac{1}{2}\right), \quad (1.5)$$

which gives

$$\Xi(t) = \frac{1}{2}\left(\frac{1}{2} + it\right)\left(-\frac{1}{2} + it\right)\pi^{-1/4-it/2}\Gamma\left(\frac{it}{2} + \frac{1}{4}\right)\zeta\left(it + \frac{1}{2}\right). \quad (1.6)$$

This function is analytic everywhere and has zeros with imaginary part between $-\frac{1}{2}$ and $\frac{1}{2}$ [BCRW08]. $\Xi(t)$ was the function originally considered and actually denoted $\xi(t)$ by Riemann himself [Edw01]. Riemann “conjectured” that all zeros α of $\Xi(t)$ are real, that is, all non-trivial zeros of the Riemann zeta function are of the form $\frac{1}{2} + i\alpha$ [BCRW08]. Since $\Xi(t)$ is even and real on the real line, stating that all zeros of $\Xi(t)$ in the first quadrant of the complex plane Q ($\text{Re}(t) \geq 0$, $\text{Im}(t) \geq 0$) are real is equivalent to the Riemann Hypothesis [Hag11].

As stated in [Hag11], the Riemann Xi function can be re-written as

$$\Xi(z) = \int_0^\infty \cos(zt)\phi(t)dt, \quad (1.7)$$

where we have only changed the variable from t to z for Ξ and $\phi(t) = \sum_{n=1}^{\infty} \phi_n(t)$

with

$$\phi_n(t) = \exp(-n^2\pi \exp(2t))(8\pi^2 n^4 \exp(\frac{9}{2}t) - 12\pi n^2 \exp(\frac{5}{2}t)). \quad (1.8)$$

Hence, $\Xi(z)$ can be simply expressed as an integral of an infinite sum of functions.

Note that if a given family of approximates approach $\Xi(z)$ uniformly, and if we can prove that, within a certain sub-region of Q , all zeros of each element in the family are real, with the size of the sub-region expanding to eventually include all of Q as the approximates approach $\Xi(z)$, then this would also imply the Riemann Hypothesis [Hag11].

After looking at related functions that closely relate to the Riemann zeta function and arriving at statements that imply the Riemann Hypothesis, we looked at the statements further. First, we looked at the following function.

From [Hag11], a hyperbolic gamma function $G(z; a, b)$ is defined as

$$G(z; a, b) = 4 \int_0^\infty \cos(2zu) \exp(2bu - a \exp(2u)) du, \quad (1.9)$$

where $z \in \mathbb{C}$, $a, b \in \mathbb{R}$ with $a > 0$. Using change of variables ($t = a \exp(2u)$,

$dt = a \exp(2u)2du$, $du = dt/2t$), as stated in [Hag11], we can re-write this as

$$G(z; a, b) = 2 \int_a^\infty \exp(b \log(t/a) - t) \cos(z \log(t/a)) \frac{dt}{t} \quad (1.10)$$

$$= \int_a^\infty (t/a)^b \exp(-t) (\exp(iz \log(t/a))) + \exp(-iz \log(t/a)) \frac{dt}{t} \quad (1.11)$$

$$= \int_a^\infty \exp(-t)((t/a)^{b+iz} + (t/a)^{b-iz}) \frac{dt}{t} \quad (1.12)$$

$$= \frac{\Gamma(b + iz, a)}{a^{b+iz}} + \frac{\Gamma(b - iz, a)}{a^{b-z}}, \quad (1.13)$$

where

$$\Gamma(z, a) = \int_a^\infty \exp(-t)t^{z-1} dt \quad (1.14)$$

is the (upper) incomplete gamma function. Note that for $a \in \mathbb{R}$, $a > 0$, $\Gamma(z, a)$ is analytic everywhere, so $G(z; a, b)$ is analytic everywhere as well [Hag11].

Using (1.7) and (1.10) as in [Hag11], $\Xi(z)$ can be re-written as

$$\Xi(z) = \sum_{n=1}^{\infty} 2\pi^2 n^4 G(z/2; n^2 \pi, 9/4) - 3\pi n^2 G(z/2; n^2 \pi, 5/4). \quad (1.15)$$

Note that since the family of approximates uniformly converge to $\Xi(z)$, we interchanged the integration and summation signs. Recall that proving all zeros of each element in the family of approximates to be real within a certain sub-region of Q implies the Riemann Hypothesis. Hence, we looked at the following Riemann Xi

approximates as defined in [Hag11]

$$\Xi_N(z) := \sum_{n=1}^N \Phi_n(z), \quad (1.16)$$

where

$$\Phi_n(z) := 2\pi^2 n^4 G(z/2; n^2\pi, 9/4) - 3\pi n^2 G(z/2; n^2\pi, 5/4). \quad (1.17)$$

Note that $\phi(t)$ from $\Xi(z)$ has been replaced by $\sum_{n=1}^N \phi_n(t)$ to obtain the Ξ approximates.

Interestingly, all of the computer runs done on Maple so far indicate that $\Xi_N(z)$ has monotonic zeros [Hag11]. That is, when we list the zeros by increasing real part, the imaginary parts of the zeros are monotone non-decreasing. Formally, if $\{\alpha_1, \alpha_2, \dots\}$ are the zeros of $\Xi_N(z)$ in a region D numbered so that $\operatorname{Re}(\alpha_i) < \operatorname{Re}(\alpha_{i+1})$ for $i \geq 1$, then $\operatorname{Im}(\alpha_i) \leq \operatorname{Im}(\alpha_{i+1})$ [Hag11]. Note that we assumed $\Xi_N(z)$ has at most one zero on the intersection of any vertical line with D [Hag11]. Hence, [Hag11] provided the following conjecture and proposition.

Conjecture 1.5. *For $N \in \mathbb{N}$, $\Xi_N(Z)$ has monotonic zeros in Q [Hag11].*

Proposition 1.6. *Conjecture 1.6 implies the Riemann Hypothesis [Hag11].*

Before looking at the proof of Proposition 1.7, we recalled the argument principle first.

Theorem 1.7. *(Argument principle) Suppose f is meromorphic in an open set con-*

taining a circle C and its interior. If f has no poles and never vanishes on C , then

$$\frac{1}{2\pi i} \int_C \frac{f'(z)}{f(z)} dz = (\text{number of zeros of } f \text{ inside } C) - (\text{number of poles of } f \text{ inside } C), \quad (1.18)$$

where the zeros and poles are counted with their multiplicities [SS03].

Then, we looked at Hardy's Theorem, which establishes the most basic/minimal necessary condition for the Riemann Hypothesis to be true.

Theorem 1.8. (*Hardy's Theorem*) *There are infinitely many zeros of $\zeta(s)$ on the line*

$$\operatorname{Re}(s) = \frac{1}{2}.$$

Proof of Prop 1.7 (from [Hag11]). The proof proves the contrapositive of the proposition. Assume that the Riemann Hypothesis is false and let $\tau = \sigma + it$ be the zero of $\Xi(z)$ in Q with minimal real part, among those zeros with positive imaginary part. By the argument principle, we have

$$\frac{1}{2\pi i} \int_{C_\epsilon} \frac{\Xi'(z)}{\Xi(z)} dz = 1, \quad (1.19)$$

where the integral is taken counterclockwise around a circle C_ϵ centered at τ , of sufficiently small radius ϵ , so no other zeros of $\Xi(z)$ are enclosed in C_ϵ . Recall that $\Xi(z)$ is analytic everywhere, so $\Xi(z)$ does not have poles. Next, we choose N sufficiently large so that $\Xi_N(z)$ has a real zero γ with $\gamma > 2\sigma$. We can do this since $\Xi_N(z)$ converges uniformly to $\Xi(z)$ in Q , both $\Xi(z)$ and $\Xi_N(z)$ are real on the real line,

and $\Xi(z)$ has infinitely many positive real zeros by Hardy's theorem. By assumption, $\Xi_N(z)$ has monotonic zeros in Q . Hence, $\Xi_N(z)$ has no non-real zeros in Q with real part less than 2σ . This implies

$$\frac{1}{2\pi i} \int_{C_\epsilon} \frac{\Xi'_N(z)}{\Xi_N(z)} dz = 0, \quad (1.20)$$

and so

$$1 = \frac{1}{2\pi i} \int_{C_\epsilon} \frac{\Xi'(z)}{\Xi(z)} - \frac{\Xi'_N(z)}{\Xi_N(z)} dz \quad (1.21)$$

$$= \frac{1}{2\pi i} \int_{C_\epsilon} \frac{\Xi'(z)\Xi_N(z) - \Xi'_N(z)\Xi(z)}{\Xi(z)\Xi_N(z)} dz. \quad (1.22)$$

On the closed and bounded set C_ϵ , $|\Xi(z)|$ is nonzero. Hence, $|\Xi(z)|$ must reach an absolute minimum on C_ϵ . Call this δ , which is positive since $|\Xi(z)| > 0$ for all $z \in C_\epsilon$. Since $\Xi_N(z)$ uniformly converges to $\Xi(z)$ as $N \rightarrow \infty$, the minimum of $|\Xi_N(z)|$ on C_ϵ must eventually be greater than $\delta/2$. Hence, for sufficiently large N , the modulus of the denominator of the integrand in (1.22) is bounded away from zero, but since $\Xi'_N(z)$ approaches $\Xi'(z)$ uniformly, the numerator approaches zero. Hence, the integral will also approach zero, a contradiction. Hence, $\Xi_N(z)$ does not have monotonic zeros in Q . \square

Remark 1.9. A weaker form of Conjecture 1.6, which still implies the Riemann Hypothesis, states that there are no non-real zeros of $\Xi_N(z)$ in Q whose real part is less than the largest real zero of $\Xi_N(z)$ [Hag11]. Computations indicate this weaker form

of Conjecture 1.6 is true at least for $N \leq 10$ [Hag11].

Taken together, we arrived that the conjecture on the monotonicity of the zeros of the Riemann Xi approximates implies the Riemann Hypothesis. To explore this conjecture further, we then looked at the zeros of incomplete gamma functions, hyperbolic gamma functions, and linear combinations of Φ_n 's, which make up the Riemann Xi approximates.

2 Zeros of the Incomplete Gamma Function

Recall that the (upper) incomplete gamma function is of the form

$$\Gamma(z, a) = \int_a^\infty \exp(-t) t^{z-1} dt \quad (2.1)$$

where $a \in \mathbb{R}$ with $a > 0$. A linear combination of the incomplete gamma functions make up the hyperbolic gamma function, whose linear combinations make up the Riemann Xi approximates.

Since the Riemann Xi approximates were conjectured to have monotonic zeros, we wanted to compute the zeros of various incomplete gamma functions and check for monotonicity. In order to find the zeros, Maple's Analytic function was used under the RootFinding package. The domain was set to be from $0+0i$ to $50+250i$ so that Maple would be able to compute the zeros in a reasonable amount of time. From [Hag11], the zeros of $\Gamma(z, a)$ in Q are known to satisfy $y \sim \frac{2}{\pi}x \ln x$ as $|z| \rightarrow \infty$ [Hag11]. However, y should be at least twice the value of $\frac{2}{\pi}x \ln x$, since this approximation only holds for large values of z , so we rounded up $\frac{4}{\pi}x \ln x$ to the nearest integer when $x = 50$.

The zeros of various incomplete gamma functions were computed, where a ranged from 0.5 to 7 in intervals of 0.5. The zeros of each incomplete gamma function turned out to be monotonic and are listed for representative incomplete gamma functions in the Appendix section.

In addition, we computed the zeros of the derivatives of incomplete gamma func-

tions used previously to see if the zeros are monotonic. If so, then this would provide evidence that the monotonicity of zeros of incomplete gamma functions is a strong property. We also checked to see if there is any interlacing between the real parts, imaginary parts, and modulus of the zeros of the incomplete gamma function and of the zeros of its derivative. If so, then this would provide evidence that the zeros have Rolle's Theorem-like property. Recall that the Rolle's Theorem states that if $f(x)$ is a real-valued continuous function on $[a, b]$, differentiable on (a, b) , and $f(a) = f(b) = 0$, then there exists a point $c \in (a, b)$ such that $f'(c) = 0$. Hence, we wanted to see if the derivative's zeros would be in between the original function's zeros, since this is true for real-valued continuous functions by the Rolle's Theorem.

The zeros of each derivative turned out to be monotonic and are listed for the derivatives of representative incomplete gamma functions in the Appendix section. From $a = 0.5$ to $a = 2$, there was interlacing between the imaginary parts and between the modulus. From $a = 2.5$ to $a = 7$, there was interlacing between the real parts, between the imaginary parts, and between the modulus. The results are summarized in Table 1 below. The zeros of the incomplete gamma function and of its derivative were graphed together and representative graphs are shown in the Appendix section.

a	Real Parts	Imaginary Parts	Modulus
0.5	No	Yes	Yes
1	No	Yes	Yes
1.5	No	Yes	Yes
2	No	Yes	Yes
2.5	Yes	Yes	Yes
3	Yes	Yes	Yes
3.5	Yes	Yes	Yes
4	Yes	Yes	Yes
4.5	Yes	Yes	Yes
5	Yes	Yes	Yes
5.5	Yes	Yes	Yes
6	Yes	Yes	Yes
6.5	Yes	Yes	Yes
7	Yes	Yes	Yes

Table 1: Interlacing of zeros of $\Gamma(a, z)$ and of its derivative

Hence, we made the following conjectures.

Conjecture 2.1. *The zeros of the incomplete gamma function and of its derivative are monotonic.*

Conjecture 2.2. *Interlacing exists between the imaginary parts and between the modulus of the zeros of the incomplete gamma function and of the zeros of its derivative for all $a \in \mathbb{R}$ with $a > 0$. In addition, there exists an $\alpha \in \mathbb{R}$ such that when $a \geq \alpha$, where $2 < \alpha \leq 2.5$, interlacing also exists between the real parts of the zeros of the incomplete gamma function and of the zeros of its derivative.*

With the zeros of the incomplete gamma function, as well as the zeros of its derivative, being monotonic, the monotonicity of zeros appears to be a strong property of the incomplete gamma function. As a result, the empirical evidence in this section provides further support for the monotonicity of the zeros of the Riemann

Ξ approximates, since linear combinations of incomplete gamma functions make up the hyperbolic gamma function, whose linear combinations make up the Riemann Ξ approximates, as shown previously. In addition, the interlacing of zeros, which gets stronger as a increases, also provides us with a glimpse into the interesting properties of the incomplete gamma function. We repeated this procedure for hyperbolic gamma functions, detailed in the next section.

3 Zeros of the Hyperbolic Gamma Function

Recall that the hyperbolic gamma function is of the form

$$G(z; a, b) = \frac{\Gamma(b + iz, a)}{a^{b+iz}} + \frac{\Gamma(b - iz, a)}{a^{b-iz}} \quad (3.1)$$

where $z \in \mathbb{C}$, $a, b \in \mathbb{R}$ with $a > 0$. A linear combination of the hyperbolic gamma functions, which is a linear combination of the incomplete gamma functions, make up the Riemann Xi approximates.

Again, we wanted to compute the zeros of various hyperbolic gamma functions and check for monotonicity. The domain was set to be from $0.01 + 0i$ to $250 + 50i$ so that Maple would be able to compute the zeros in a reasonable amount of time. From [Hag11], the zeros of $G(z; a, b)$ in Q are known to satisfy $x \sim \frac{2}{\pi}y \ln y$ as $|z| \rightarrow \infty$ [Hag11]. However, x should be at least twice the value of $\frac{2}{\pi}y \ln y$, since this approximation only holds for large values of z , so we rounded up $\frac{4}{\pi}y \ln y$ to the nearest integer when $y = 50$.

The zeros of various hyperbolic gamma functions were computed, where a ranged from 1.5 to 3.5 in intervals of 0.5 and b ranged from -5 to 7 in intervals of 0.5. The zeros of each hyperbolic gamma function turned out to be monotonic and are listed for representative hyperbolic gamma functions in the Appendix section.

Although the zeros of the hyperbolic gamma functions in different regions of Q were all monotonic in several hundred computer runs, [Hag11] indicated that there

exist hyperbolic gamma functions with non-monotonic zeros. In [Hag11], it has been shown that as $z \rightarrow \infty$ along the positive real line, the hyperbolic gamma function can be approximated as

$$G(x; a, b) = \frac{2(a - b)}{e^a} \frac{1}{x^2} + O\left(\frac{1}{x^4}\right). \quad (3.2)$$

Hence for large x , we have $G(x; a, 2a) < 0$ and $G(x; a, 0) > 0$, so there must exist some value of b , $0 < b < 2a$ for which $G(x; a, b) = 0$ [Hag11]. If this is the case, then x will be a real zero of $G(z; a, b)$, which occurs after many non-real zeros, so the zeros of $G(z; a, b)$ will not be monotonic.

In order to find numerical solutions of b for which $G(x; a, b) = 0$, we plotted $G(x; a, b)$ with respect to b , where x was set to equal four arbitrary large real numbers ($10^6, 8^{10}, 9^{10}, 10^{10}$) and a was set to range from 1.5 to 3.5 in intervals of 0.5. The number of digits was set to 100 for accuracy of the values. From graphing $G(x; a, b)$, we found out that all graphs were linearly decreasing and $G(x; a, b) = 0$ only when $a \simeq b$. The following four graphs of $G(x; a, b)$ where $a = 1.5$ in Figure 1 illustrate the results.

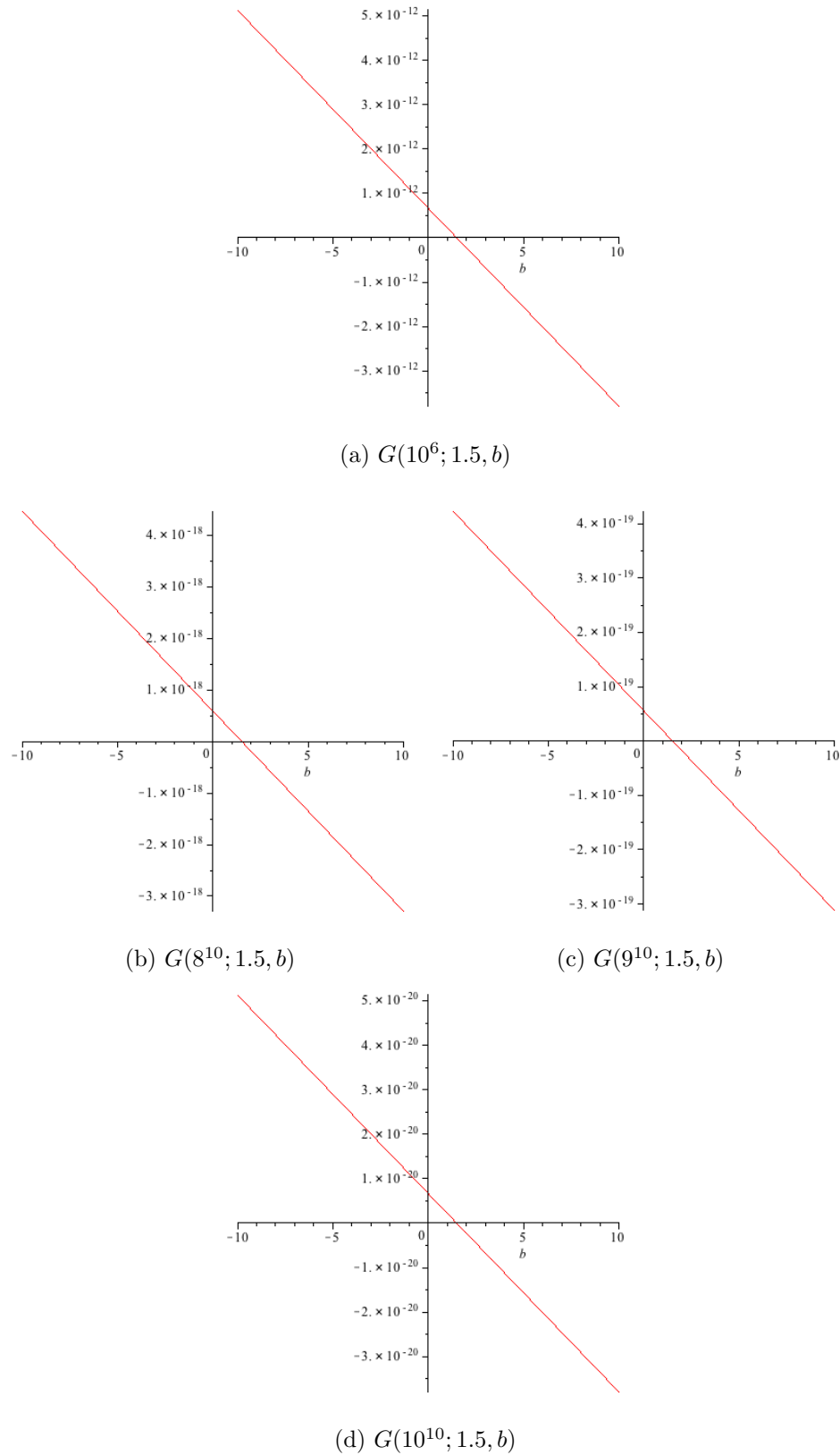


Figure 1: Graphs of $G(x; 1.5, b)$ where x is real and large

Next, we wanted to test whether we can really find a large x such that $G(x; a, b) = 0$ for any a and positive b . Hence, we plotted $G(x; a, b)$ with respect to x , where x ranged from 10^6 and a and b were set to equal arbitrary real positive numbers. Again, the number of digits was set to 100 for accuracy of the values. From graphing $G(x; a, b)$, we found out that none of the graphs had points such that $G(x; a, b) = 0$. Interestingly, the graph of $G(x; a, b)$, where x was large, resembled an exponentially decreasing curve when $b < a$ and resembled an asymptotically increasing curve when $b \geq a$. The following four graphs of $G(x; a, b)$ where $a = 1.5$ in Figure 2 illustrate this.

Finally, we wanted to test whether we can find a large x such that $G(x; a, b) = 0$ for any a and non-positive b . Hence, we plotted $G(x; a, b)$ with respect to x , where x ranged from 10^6 and a and b were set to equal arbitrary real positive numbers and non-positive numbers, respectively. Again, the number of digits was set to 100 for accuracy of the values, and there were no points such that $G(x; a, b) = 0$ for all graphs. Since $b < a$ in this case, the graph of $G(x; a, b)$, where x was large, resembled an exponentially decreasing curve, consistent with the previous results when $b < a$. The following four graphs of $G(x; a, b)$ where $a = 1.5$ in Figure 3 illustrate the results.

Taken together, these results indicated that $G(z; a, b)$ had a large real zero x only when $a \simeq b$. This implies that the hyperbolic gamma function has non-monotonic zeros when $a \simeq b$, since $G(x; a, b) = 0$ indicates the presence of a large real zero after many non-real zeros.

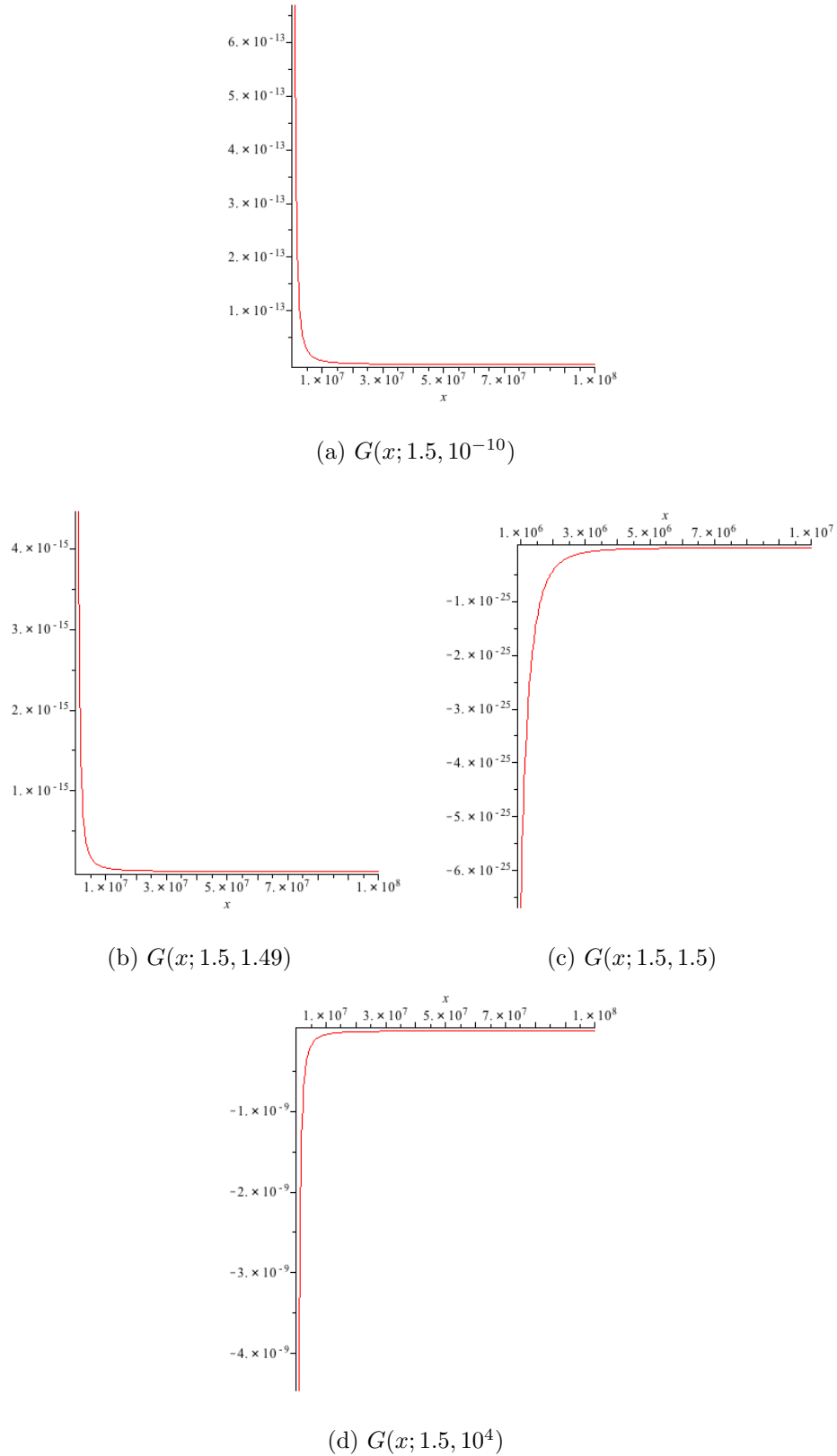
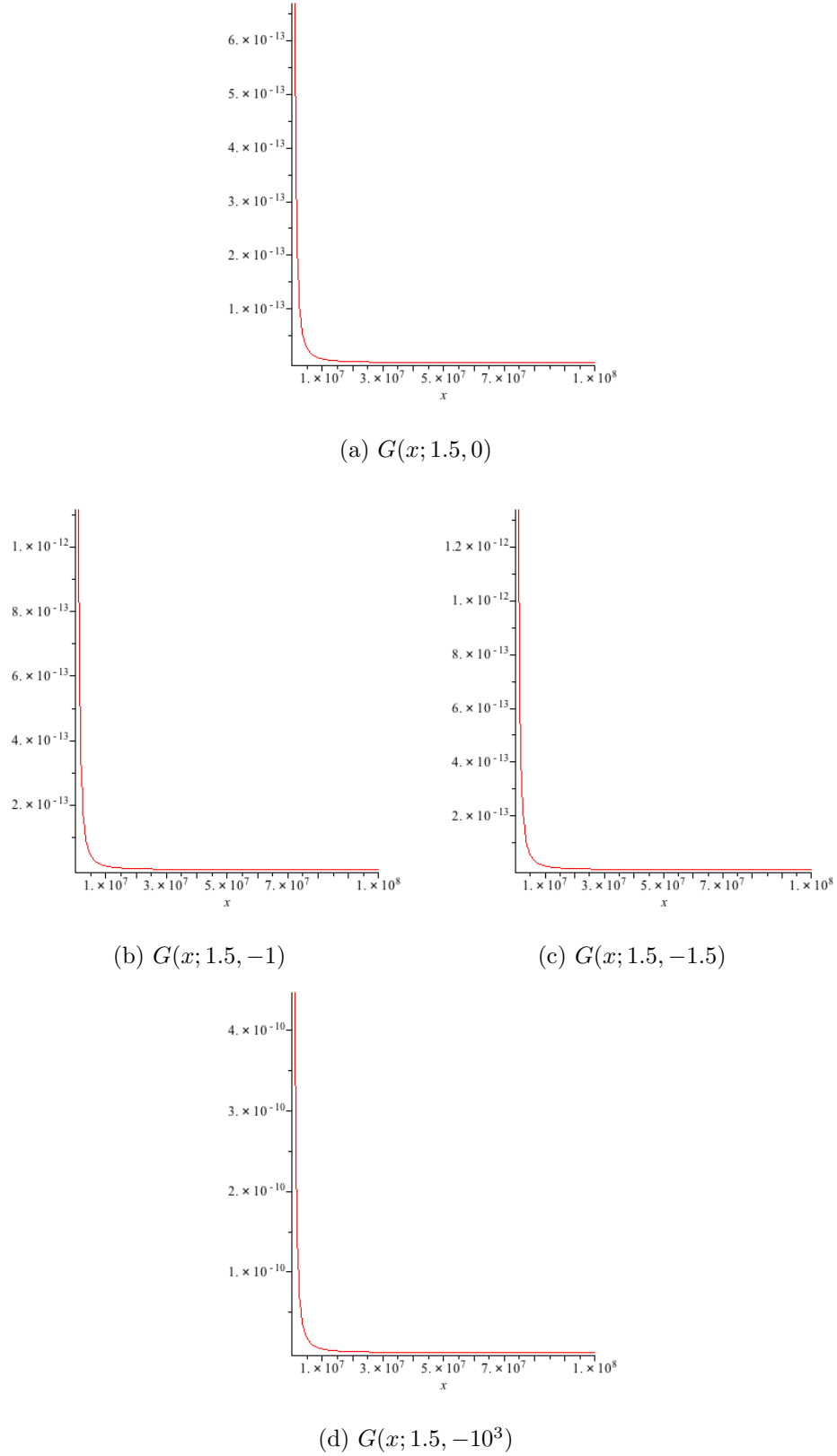


Figure 2: Graphs of $G(x; 1.5, b)$ where b is positive

Figure 3: Graphs of $G(x; 1.5, b)$ where b is non-positive

Hence, we made the following conjecture.

Conjecture 3.1. *The zeros of the hyperbolic gamma function are monotonic when $a \neq b$.*

Although the zeros were monotonic for tested hyperbolic gamma functions where $a = b$, the region in which the zeros were computed was nowhere near the large x values for which $G(x; a, b) = 0$.

In addition, we observed that the zero of $G(z; a, b)$ in Q with the smallest modulus was real when b was approximately equal to or greater than a . More specifically, the lower bound for b for which the zero with the smallest modulus is real approached a as a increased. For example, for $a = 1.5$, b had to be greater than $0.86a$ for the zero with the smallest modulus to be real, whereas for $a = 2$, b had to be greater than $0.9a$. The lower bounds were calculated by graphing $G(z; a, b)$ with respect to z , where z was a real number ranging from 0 to 10, a ranged from 1.5 to 3.5 in intervals of 0.5, and b was set to arbitrary real numbers. As b increased, the graph “lowered down” and crossed the horizontal axis after a certain point. The smallest crossing point corresponded to the zero with the smallest modulus for that particular a and b , which was real. The results are summarized in Table 2 below.

a	Lower bound for b
1.5	$0.86a$
2	$0.9a$
2.5	$0.924a$
3	$0.9367a$
3.5	$0.94857a$

Table 2: Lower bound for b for which the zero of $G(z; a, b)$ with the smallest

modulus is real

Furthermore, we computed the zeros of the derivatives of hyperbolic gamma functions used previously to see if the zeros are monotonic. If so, then this would provide evidence that the monotonicity of zeros of hyperbolic gamma functions is a strong property. However, the zeros of few derivatives were not able to be computed within two days (e.g. for $a = 1.5$ and $b = 4, 6, 6.5$). The zeros of each derivative turned out to be monotonic and are listed for the derivatives of representative hyperbolic gamma functions in the Appendix section. However, the zeros of the derivatives of hyperbolic gamma functions where $a \simeq b$ might not be monotonic, like the zeros of the original function, when computed in a bigger region. Hence, this needs to be tested to conclude that the derivatives of hyperbolic gamma functions where $a \simeq b$ have monotonic zeros or not.

We also checked to see if there is any interlacing between the real parts, imaginary parts, and modulus of the zeros of the hyperbolic gamma function and of the zeros of its derivative. Again, we wanted to see if the derivative's zeros would be in between the original function's zeros and have a Rolle's Theorem-like property. For most functions, including when $b \leq 0$ and $b < a$, there was interlacing between the real parts and between the modulus, but no interlacing between the imaginary parts. For rest of the functions, interlacing did not exist at all. The results are summarized in the Appendix section. The zeros of a hyperbolic gamma function and of its derivative were graphed together and representative graphs are shown in the Appendix section.

Hence, we made the following conjectures.

Conjecture 3.2. *The zeros of the derivative of hyperbolic gamma function are monotonic when $a \neq b$.*

Conjecture 3.3. *There exists an $\alpha \in \mathbb{R}$ such that when $b \leq \alpha$, where $0 < \alpha < a$, interlacing exists between the real parts and between the modulus of the zeros of the hyperbolic gamma function and of the zeros of its derivative for all $a \in \mathbb{R}$ with $a > 0$.*

With the zeros of the hyperbolic gamma function, as well as the zeros of its derivative, being monotonic when $a \neq b$, the monotonicity of zeros appears to be a strong property of the hyperbolic gamma function, like the incomplete gamma function. As a result, the empirical evidence in this section provides further support for the monotonicity of the zeros of the Riemann Xi approximates, since linear combinations of hyperbolic gamma functions make up the Riemann Xi approximates, as shown previously. It is interesting that there is no interlacing between the imaginary parts of zeros for the hyperbolic gamma function, even though the incomplete gamma function had it for all $a \in \mathbb{R}$ with $a > 0$. We repeated this procedure once more for linear combinations of Φ_n 's, detailed in the next section.

4 Zeros of the Linear Combination of Φ_n 's

Recall that the Riemann Xi approximate is of the form

$$\Xi_N(z) := \sum_{n=1}^N \Phi_n(z), \quad (4.1)$$

where

$$\Phi_n(z) := 2\pi^2 n^4 G(z/2; n^2\pi, 9/4) - 3\pi n^2 G(z/2; n^2\pi, 5/4). \quad (4.2)$$

Hence, the Riemann Xi approximate is simply a finite sum of Φ_n 's. It has already been conjectured that the Riemann Xi approximate has monotonic zeros. Hence, we wanted to check whether linear combinations of Φ_n 's, where not all of the Φ_n 's have a coefficient of 1, have monotonic zeros.

To introduce the ultimate motivation for this problem, the following definition and proposition need to be defined.

Definition 4.1. A family $\{f_1(z), \dots, f_k(z)\}$ of polynomials with real coefficients is called compatible if $\sum_{j=1}^k c_j f_j(z)$ has only real zeros whenever $c_j \in \mathbb{R}$, $c_j \geq 0$ for $1 \leq j \leq k$. It is called pairwise compatible if $\{f_i, f_j\}$ forms a compatible family for each pair $1 \leq i < j \leq k$ [Hag11].

Proposition 4.2. *Let f_1, \dots, f_k be polynomials with positive leading coefficients and all roots real. Then f_1, \dots, f_k being pairwise compatible is equivalent to f_1, \dots, f_k being compatible [CS07].*

In [Hag11], it has been questioned whether a similar statement holds if we replace real polynomials with positive leading coefficients and only real zeros, by even, real, entire functions having monotonic zeros in Q . However, we do not know whether any series of the form $\sum_{k=1}^N c_k \Phi_k(z)$, where $c_k \in \mathbb{R}$ with $c_k \geq 0$, even has monotonic zeros. Hence, this needed to be tested first in order to tackle the big question. From [Hag11], it has been advised that $c_1 = 1$ and $0 \leq c_i \leq 1$ for $i > 1$ to avoid non-monotonic zeros.

As a result, zeros of fourteen different linear combinations of Φ_n 's with the above condition were computed and checked for monotonicity. The domain was set to be from $0.01 + 0i$ to $250 + 50i$ so that Maple would be able to compute the zeros in a reasonable amount of time. From [Hag11], the zeros of any function of the form $\sum_{k=1}^N u_k G(z; a_k, b_k)$, where $a_k, b_k \in \mathbb{R}$, $u_k \in \mathbb{C}$, $a_k > 0$, in Q are known to satisfy $x \sim \frac{2}{\pi} y \ln y$ as $|z| \rightarrow \infty$ [Hag11]. However, x should be at least twice the value of $\frac{2}{\pi} y \ln y$, since this approximation only holds for large values of z , so we rounded up $\frac{4}{\pi} y \ln y$ to the nearest integer when $y = 50$. The zeros of each linear combination of Φ_n 's turned out to be monotonic and are listed in the Appendix section.

In addition, we attempted to compute the zeros of the derivatives of linear combinations of Φ_n 's previously used to see if the zeros are monotonic. If so, then this would provide evidence that the monotonicity of zeros of liner combinations of Φ_n 's is a strong property. However, Maple was not able to compute the zeros in a reasonable amount of time. As a result, an alternative method introduced in [Hag11] needs to

be used to compute the zeros of the derivatives. The alternative method is outlined as follows.

Recall that Riemann “conjectured” that all zeros α of $\Xi(z)$ are real. This is equivalent to the statement that the modulus of $\Xi(z)$ is monotone increasing along any vertical ray which starts at a point $x \geq 0$ on the non-negative real line and travels straight upward to $x + i\infty$ [Hag11]. To see why this is true, first recall a few definitions.

Definition 4.3. Let f be an entire function. If there exist a positive number ρ and constants $A, B > 0$ such that $|f(z)| \leq A \exp(B|z|^\rho)$ for all $z \in \mathbb{C}$, then we say that f has an order of growth $\leq \rho$. We define the order of growth of f as $\rho_f = \inf \rho$, where the infimum is over all $\rho > 0$ such that f has an order of growth $\leq \rho$ [SS03].

Definition 4.4. For each integer $k \geq 0$ we define canonical factors by $E_0(z) = 1 - z$ and $E_k(z) = (1 - z) \exp(z + z^2/2 + \dots + z^k/k)$, for $k \geq 1$. The integer k is called the degree of the canonical factor [SS03].

Now recall Hadamard’s factorization theorem.

Theorem 4.5. Suppose f is entire and has growth order ρ_0 . Let k be the integer so that $k \leq \rho_0 < k + 1$. If a_1, a_2, \dots denote the (non-zero) zeros of f , then

$$f(z) = \exp(P(z)) z^m \prod_{n=1}^{\infty} E_k(z/a_n), \quad (4.3)$$

where P is a polynomial of degree $\leq k$, and m is the order of the zero of f at $z = 0$.

[SS03].

Using Hadamard's factorization theorem, the modulus of $\Xi(z)$ can be written as

$$|\Xi(z)| = |\Xi(0)| \prod_i |1 - z^2/\alpha_i^2|, \quad (4.4)$$

where the α_i 's are the positive real zeros of $\Xi(z)$ [Hag11]. Then as stated in [Hag11],

we can take the partial derivative of equation (4.4) with respect to y , where $z = x + iy$,

and get

$$\frac{\partial}{\partial y} |\Xi(z)| = |\Xi(0)| \frac{\partial}{\partial y} \exp\left(\sum_{i=1}^{\infty} \ln(1 - z^2/\alpha_i^2)\right) \quad (4.5)$$

$$= |\Xi(0)| \exp\left(\sum_{i=1}^{\infty} \ln(1 - z^2/\alpha_i^2)\right) \frac{\partial}{\partial y} \sum_{i=1}^{\infty} \ln(1 - z^2/\alpha_i^2) \quad (4.6)$$

$$= |\Xi(0)| \exp\left(\sum_{i=1}^{\infty} \ln(1 - z^2/\alpha_i^2)\right) \sum_{i=1}^{\infty} \frac{1}{1 - z^2/\alpha_i^2} \left(\frac{4y}{\alpha_i^2}(1 + \frac{y^2}{\alpha_i^2})\right). \quad (4.7)$$

Hence, equation (4.7) is positive for positive y and indeed, $|\Xi(z)|$ is monotone increasing along any vertical ray if the Riemann Hypothesis is true.

Now for a given function $F(z)$, analytic in Q , and α a non-negative real number, let $M(F, \alpha)$ denote the value of $y \geq 0$ where the function $|F(\alpha + iy)|$ is minimal [Hag11]. If this minimum occurs at more than one y , let $M(F, \alpha)$ denote the infimum of such y [Hag11]. We can calculate $M(F, \alpha)$ by calculating $|F(\alpha + iy)|$ at many closely spaced grid points y and then choose the y that gives the minimum [Hag11]. From [Hag11], it has been noted that the modulus of a sum of hyperbolic gamma

functions increases rapidly when y increases beyond a certain point.

In addition, let the set of pairs $\{(\alpha, M(F, \alpha))\}$ in Q denote the “ M -curve” of F [Hag11]. When the M -curve is plotted on a grid using Maple, it resembles a continuous curve and has the property that the non-real zeros of F in Q occur at the same places as the local maxima of the M -curve [Hag11]. Hence, this is another method to calculate the zeros of the derivatives of the linear combinations of Φ_n ’s.

To support this method further, [Hag11] shows why the local maximums of the M -curve are linked to the zeros of F . Assume that $|F(\alpha + iy)|$, $y \geq 0$, is monotone decreasing in y until it reaches a certain minimum and then is monotone increasing afterwards [Hag11]. Let $F = u(x, y) + iv(x, y)$ and take the partial derivative of $|F(\alpha + iy)|^2 = u^2 + v^2$ with respect to y [Hag11]. Then set the partial derivative equal to 0, since we are concerned with the M -curve, which consists of points $y \geq 0$ where $|F(\alpha + iy)|$ is minimal. Then we get

$$uu_y + vv_y = 0. \quad (4.8)$$

Now as stated in [Hag11], assume that the Implicit Function Theorem also holds. Then equation (4.8) implicitly defines y as a function of x [Hag11]. So we can take the derivative of equation (4.8) with respect to x and get

$$u_x u_y + uu_{yx} + (u_y u_y + uu_{yy})y' + v_x v_y + vv_{yx} + (v_y v_y + vv_{yy})y' = 0. \quad (4.9)$$

Now assume that $z = \alpha + iy$ is a zero of F . Then when we plug in z to F , we get

$|F(\alpha + iy)|^2 = u^2 + v^2 = 0 \Rightarrow u = v = 0$. As a result, equation (4.9) simplifies to

$$u_x u_y + v_x v_y + (u_y^2 + v_y^2)y' = 0. \quad (4.10)$$

Finally as stated in [Hag11], use the Cauchy-Riemann equations ($u_x = v_y, u_y = -v_x$)

and get

$$(u_y^2 + v_y^2)y' = 0. \quad (4.11)$$

Hence, we get that $y' = 0$, since $u_y = v_y = 0$ would imply that F is constant [Hag11].

Hence, since $y' = 0$, $z = \alpha + iy$ is a local maximum of the M -curve, as well as a zero of F .

Taken together, the M -curve method should be attempted to calculate the zeros of the derivatives of linear combinations of Φ_n 's. Then we will be able to conclude that the derivatives of linear combinations of Φ_n 's have monotonic zeros or not. Moreover, we will be able to check whether there is any interlacing between the real parts, imaginary parts, and modulus of the zeros of the linear combination of Φ_n 's and of the zeros of its derivative. As a result, more work needs to be done on the linear combinations of Φ_n 's. Ultimately, we hope that the findings and results from the linear combinations of Φ_n 's will support the Riemann Xi approximates having monotonic zeros.

5 Appendix

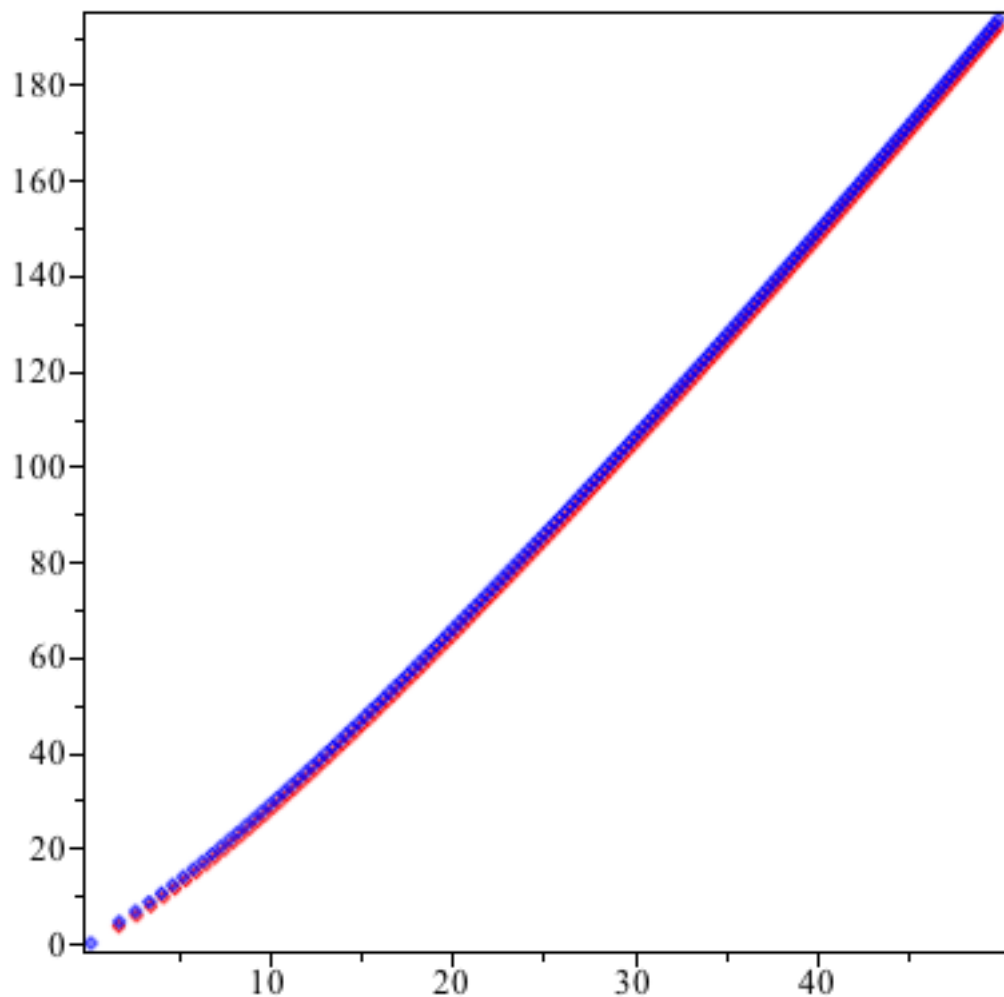


Figure 4: Zeros of $\Gamma(z, 0.5)$ in red and of its derivative in blue

Zeros of $\Gamma(z, 0.5)$ in rectangle with corners (0,0), (50,250).

```

1.746623662+3.509431123*I,
2.715124825+5.754064220*I,
3.502197402+7.753272095*I,
4.195286003+9.616964790*I,
4.827998540+11.38962033*I,
5.417532345+13.09492246*I,
5.974108640+14.74739962*I,
6.504400310+16.35678636*I,
7.013055325+17.93001392*I,
7.503468920+19.47224236*I,
7.978213290+20.98744659*I,
8.439294125+22.47877231*I,
8.888312450+23.94876428*I,
9.326571255+25.39951873*I,
9.755148440+26.83278909*I,
10.17494819+28.25006126*I,
10.58673815+29.65260872*I,
10.99117691+31.04153371*I,
11.38883477+32.41779849*I,
11.78020958+33.78224966*I,
12.16573920+35.13563714*I,
12.54581115+36.47862934*I,
12.92077061+37.81182532*I,
13.29092653+39.13576476*I,
13.65655690+40.45093599*I,
14.01791301+41.75778295*I,
14.37522277+43.05671049*I,
14.72869388+44.34808941*I,
15.07851620+45.63226029*I,
15.42486383+46.90953700*I,
15.76789696+48.18020957*I,
16.10776335+49.44454674*I,
16.44459968+50.70279815*I,
16.77853270+51.95519620*I,
17.10968019+53.20195780*I,
17.43815189+54.44328570*I,
17.76405022+55.67936985*I,
18.08747096+56.91038860*I,
18.40850385+58.13650960*I,
18.72723312+59.35789065*I,
19.04373797+60.57468075*I,

```

19.35809295+61.78702050*I,
19.67036838+62.99504295*I,
19.98063067+64.19887425*I,
20.28894259+65.39863375*I,
20.59536362+66.59443505*I,
20.89995010+67.78638605*I,
21.20275554+68.97458940*I,
21.50383076+70.15914300*I,
21.80322413+71.34014010*I,
22.10098168+72.51766985*I,
22.39714730+73.69181725*I,
22.69176287+74.86266385*I,
22.98486837+76.03028750*I,
23.27650201+77.19476290*I,
23.56670036+78.35616155*I,
23.85549843+79.51455220*I,
24.14292974+80.67000085*I,
24.42902645+81.82257080*I,
24.71381943+82.97232300*I,
24.99733831+84.11931615*I,
25.27961156+85.26360670*I,
25.56066657+86.40524905*I,
25.84052967+87.54429565*I,
26.11922624+88.68079715*I,
26.39678070+89.81480235*I,
26.67321666+90.94635840*I,
26.94855670+92.07551090*I,
27.22282287+93.20230390*I,
27.49603629+94.32678000*I,
27.76821742+95.44898045*I,
28.03938600+96.56894520*I,
28.30956114+97.68671290*I,
28.57876134+98.80232100*I,
28.84700448+99.91580585*I,
29.11430788+101.0272026*I,
29.38068833+102.1365456*I,
29.64616210+103.2438680*I,
29.91074493+104.3492019*I,
30.17445214+105.4525787*I,
30.43729857+106.5540287*I,
30.69929860+107.6535816*I,
30.96046624+108.7512661*I,

31.22081506+109.8471102*I,
31.48035828+110.9411412*I,
31.73910874+112.0333854*I,
31.99707889+113.1238687*I,
32.25428089+114.2126162*I,
32.51072654+115.2996524*I,
32.76642734+116.3850013*I,
33.02139449+117.4686860*I,
33.27563889+118.5507292*I,
33.52917116+119.6311532*I,
33.78200162+120.7099799*I,
34.03414044+121.7872290*I,
34.28559738+122.8629225*I,
34.53638205+123.9370800*I,
34.78650384 + 125.0097212 I,
35.03597184 + 126.0808653 I,
35.28479499 + 127.1505310 I,
35.53298199 + 128.2187365 I,
35.78054134 + 129.2854999 I,
36.02748148 + 130.3508387 I,
36.27381010 + 131.4147697 I,
36.51953555 + 132.4773101 I,
36.76466543 + 133.5384761 I,
37.00920732 + 134.5982838 I,
37.25316862 + 135.6567488 I,
37.49655659 + 136.7138866 I,
37.73937830 + 137.7697122 I,
37.98164068 + 138.8242404 I,
38.22335050 + 139.8774857 I,
38.46451449 + 140.9294622 I,
38.70513906 + 141.9801838 I,
38.94523062 + 143.0296641 I,
39.18479535 + 144.0779165 I,
39.42383950 + 145.1249540 I,
39.66236893 + 146.1707895 I,
39.90038954 + 147.2154356 I,
40.13790709 + 148.2589046 I,
40.37492720 + 149.3012087 I,
40.61145542 + 150.3423597 I,
40.84749716 + 151.3823693 I,
41.08305773 + 152.4212490 I,
41.31814236 + 153.4590100 I,

41.55275615 + 154.4956634 I,
 41.78690412 + 155.5312200 I,
 42.02059121 + 156.5656905 I,
 42.25382224 + 157.5990854 I,
 42.48660197 + 158.6314149 I,
 42.71893506 + 159.6626893 I,
 42.95082608 + 160.6929183 I,
 43.18227952 + 161.7221118 I,
 43.41329981 + 162.7502794 I,
 43.64389127 + 163.7774306 I,
 43.87405818 + 164.8035745 I,
 44.10380471 + 165.8287204 I,
 44.33313499 + 166.8528773 I,
 44.56205305 + 167.8760539 I,
 44.79056288 + 168.8982589 I,
 45.01866838 + 169.9195010 I,
 45.24637340 + 170.9397886 I,
 45.47368171 + 171.9591298 I,
 45.70059704 + 172.9775330 I,
 45.92712303 + 173.9950060 I,
 46.15326330 + 175.0115569 I,
 46.37902136 + 176.0271933 I,
 46.60440072 + 177.0419230 I,
 46.82940479 + 178.0557534 I,
 47.05403694 + 179.0686922 I,
 47.27830050 + 180.0807464 I,
 47.50219874 + 181.0919234 I,
 47.72573486 + 182.1022303 I,
 47.94891204 + 183.1116741 I,
 48.17173339 + 184.1202616 I,
 48.39420199 + 185.1279997 I,
 48.61632060 + 186.1348952 I,
 48.83809299 + 187.1409543 I,
 49.05952130 + 188.1461839 I,
 49.28060869 + 189.1505903 I,
 49.50135799 + 190.1541798 I,
 49.72177204 + 191.1569588 I,
 49.94185358 + 192.1589332 I

Zeros of the derivative of $\Gamma(z, 0.5)$ in rectangle with corners (0,0), (50,250).

.2173610855,
 1.776890301+4.480266640*I,

2.669524875+6.679777750*I,
3.418173563+8.643600690*I,
4.087332409+10.47969358*I,
4.703445928+12.23006990*I,
5.280668265+13.91684528*I,
5.827684785+15.55355158*I,
6.350301055+17.14926362*I,
6.852634620+18.71045747*I,
7.337736330+20.24196773*I,
7.807944120+21.74752936*I,
8.265098290+23.23010661*I,
8.710679420+24.69210392*I,
9.145900535+26.13550703*I,
9.571770840+27.56198085*I,
9.989141090+28.97293940*I,
10.39873669+30.36959704*I,
10.80118237+31.75300681*I,
11.19702087+33.12408968*I,
11.58672747+34.48365723*I,
11.97072125+35.83242944*I,
12.34937407+37.17104898*I,
12.72301781+38.50009261*I,
13.09195019+39.82008052*I,
13.45643953+41.13148403*I,
13.81672875+42.43473196*I,
14.17303861+43.73021592*I,
14.52557051+45.01829485*I,
14.87450878+46.29929878*I,
15.22002272+47.57353204*I,
15.56226820+48.84127619*I,
15.90138920+50.10279225*I,
16.23751901+51.35832285*I,
16.57078135+52.60809415*I,
16.90129132+53.85231715*I,
17.22915619+55.09118945*I,
17.55447619+56.32489615*I,
17.87734511+57.55361110*I,
18.19785088+58.77749795*I,
18.51607611+59.99671075*I,
18.83209848+61.21139500*I,
19.14599118+62.42168810*I,
19.45782327+63.62772015*I,

19.76766002+64.82961445*I,
20.07556316+66.02748790*I,
20.38159116+67.22145165*I,
20.68579949+68.41161135*I,
20.98824083+69.59806760*I,
21.28896523+70.78091630*I,
21.58802028+71.96024895*I,
21.88545153+73.13615280*I,
22.18130209+74.30871150*I,
22.47561331+75.47800490*I,
22.76842465+76.64410950*I,
23.05977382+77.80709855*I,
23.34969692+78.96704245*I,
23.63822851+80.12400860*I,
23.92540173+81.27806190*I,
24.21124834+82.42926460*I,
24.49579886+83.57767665*I,
24.77908257+84.72335575*I,
25.06112763+85.86635740*I,
25.34196113+87.00673520*I,
25.62160911+88.14454080*I,
25.90009669+89.27982390*I,
26.17744804+90.41263270*I,
26.45368648+91.54301365*I,
26.72883451+92.67101155*I,
27.00291382+93.79666990*I,
27.27594539+94.92003065*I,
27.54794946+96.04113445*I,
27.81894561+97.16002065*I,
28.08895279+98.27672735*I,
28.35798930+99.39129160*I,
28.62607288+100.5037492*I,
28.89322072+101.6141348*I,
29.15944945+102.7224823*I,
29.42477517+103.8288243*I,
29.68921360+104.9331926*I,
29.95277983+106.0356182*I,
30.21548861+107.1361311*I,
30.47735424+108.2347605*I,
30.73839059+109.3315348*I,
30.99861120+110.4264815*I,
31.25802902+111.5196277*I,

31.51665695+112.6109994*I,
31.77450732+113.7006221*I,
32.03159219+114.7885208*I,
32.28792327+115.8747214*I,
32.54351203+116.9592420*I,
32.79836954+118.0421111*I,
33.05250682+119.1233494*I,
33.30593389+120.2029787*I,
33.55866156+121.2810203*I,
33.81069968+122.3574952*I,
34.06205837+123.4324248*I,
34.31274615+124.5058255*I
34.56277332+125.5777203*I,
34.81214864+126.6481269*I,
35.06088096+127.7170639*I,
35.30897905+128.7845494*I,
35.55645102+129.8506011*I,
35.80330547+130.9152365*I,
36.04955033+131.9784723*I,
36.29519350+133.0403253*I,
36.54024268+134.1008116*I,
36.78470542+135.1599472*I,
37.02858906+136.2177476*I,
37.27190082+137.2742281*I,
37.51464774+138.3294035*I,
37.75683673+139.3832885*I,
37.99847454+140.4358974*I,
38.23956777+141.4872443*I,
38.48012290+142.5373428*I,
38.72014627+143.5862066*I,
38.95964408+144.6338487*I,
39.19862242+145.6802823*I,
39.43708724+146.7255199*I,
39.67504438+147.7695741*I,
39.91249957+148.8124572*I,
40.14945842+149.8541810*I,
40.38592643+150.8947575*I,
40.62190899+151.9341982*I,
40.85741140+152.9725144*I,
41.09243886+154.0097174*I,
41.32699645+155.0458180*I,
41.56108917+156.0808271*I,

41.79472193+157.1147551*I,
42.02789954+158.1476126*I,
42.26062673+159.1794096*I,
42.49290818+160.2101563*I,
42.72474834+161.2398625*I,
42.95615179+162.2685378*I,
43.18712289+163.2961919*I,
43.41766597+164.3228340*I,
43.64778527+165.3484735*I,
43.87748496+166.3731193*I,
44.10676934+167.3967807*I,
44.33564183+168.4194654*I,
44.56410701+169.4411831*I,
44.79216856+170.4619420*I,
45.01983031+171.4817504*I,
45.24709604+172.5006166*I,
45.47396944+173.5185485*I,
45.70045415+174.5355542*I,
45.92655377+175.5516416*I,
46.15227182+176.5668183*I,
46.37761176+177.5810920*I,
46.60257702+178.5944702*I,
46.82717096+179.6069602*I,
47.05139687+180.6185692*I,
47.27525803+181.6293046*I,
47.49875761+182.6391732*I,
47.72189881+183.6481821*I,
47.94468472+184.6563382*I,
48.16711839+185.6636481*I,
48.38920286+186.6701186*I,
48.61094108+187.6757561*I,
48.83233598+188.6805672*I,
49.05339044+189.6845582*I,
49.27410732+190.6877354*I,
49.49448939+191.6901051*I,
49.71453943+192.6916732*I,
49.93426014+193.6924460*I

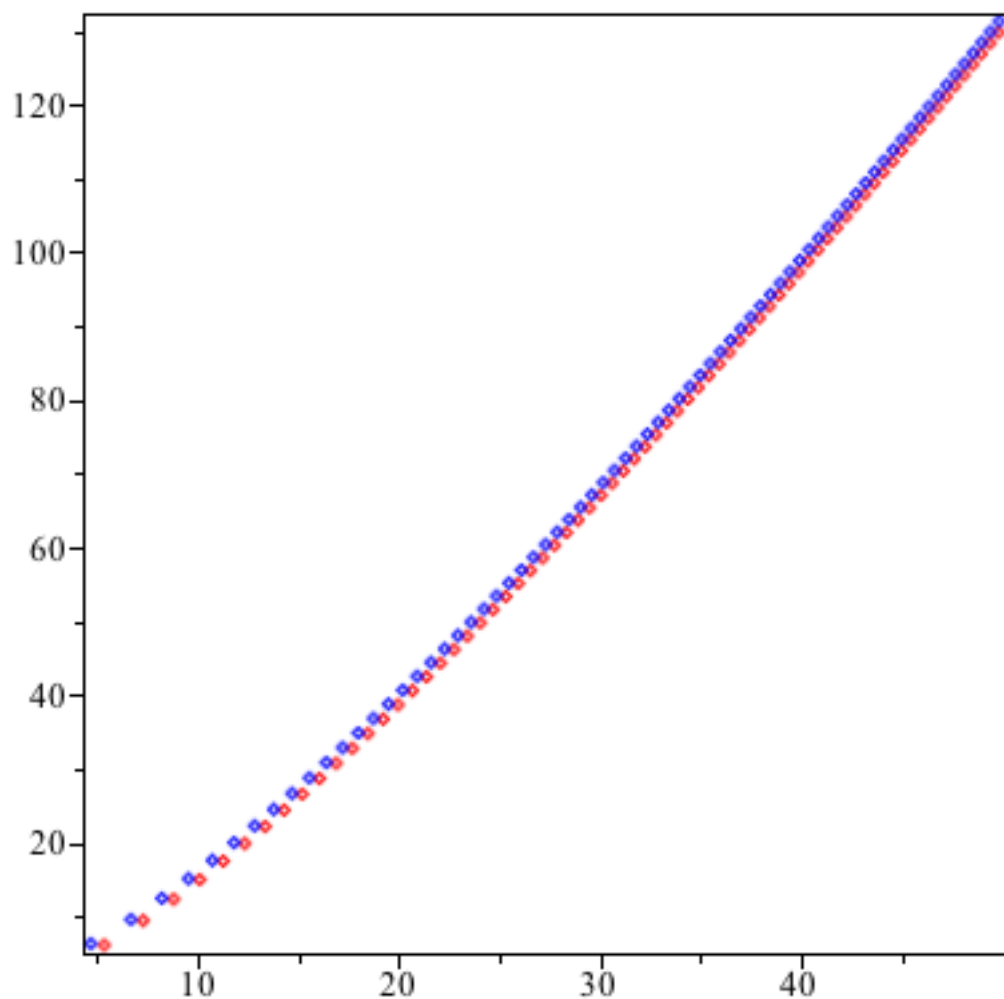


Figure 5: Zeros of $\Gamma(z, 2.5)$ in red and of its derivative in blue

Zeros of $\Gamma(z, 2.5)$ in rectangle with corners (0,0), (50,250).

```

5.336520625+6.105954720*I,
7.278037125+9.433072415*I,
8.791805325+12.32873262*I,
10.09279767+14.98879263*I,
11.26029108+17.49212126*I,
12.33389394+19.88044659*I,
13.33675256+22.17920907*I,
14.28378130+24.40535896*I,
15.18525827+26.57090361*I,
16.04862413+28.68474050*I,
16.87947200+30.75369458*I,
17.68213356+32.78314584*I,
18.46004534+34.77743088*I,
19.21598885+36.74011005*I,
19.95225355+38.67415217*I,
20.67075111+40.58206581*I,
21.37309765+42.46599502*I,
22.06067424+44.32779077*I,
22.73467238+46.16906508*I,
23.39612866+47.99123289*I,
24.04595174+49.79554487*I,
24.68494349+51.58311340*I,
25.31381594+53.35493350*I,
25.93320476+55.11189985*I,
26.54368038+56.85482055*I,
27.14575703+58.58442885*I,
27.73990026+60.30139255*I,
28.32653317+62.00632205*I,
28.90604170+63.69977735*I,
29.47877908+65.38227370*I,
30.04506957+67.05428640*I,
30.60521175+68.71625540*I,
31.15948129+70.36858875*I,
31.70813332+72.01166595*I,
32.25140460+73.64584055*I,
32.78951524+75.27144275*I,
33.32267039+76.88878165*I,
33.85106160+78.49814690*I,
34.37486806+80.09981060*I,
34.89425768+81.69402860*I,
35.40938814+83.28104210*I,

```

35.92040765+84.86107865*I,
 36.42745580+86.43435325*I,
 36.93066425+88.00106945*I,
 37.43015731+89.56141995*I,
 37.92605256+91.11558770*I,
 38.41846132+92.66374640*I,
 38.90748911+94.20606125*I,
 39.39323608+95.74268950*I,
 39.87579740+97.27378100*I,
 40.35526358+98.79947865*I,
 40.83172079+100.3199189*I,
 41.30525117+101.8352322*I,
 41.77593306+103.3455432*I,
 42.24384112+104.8509714*I,
 42.70904728+106.3516311*I,
 43.17161948+107.8476320*I,
 43.63162330+109.3390795*I,
 44.08912142+110.8260745*I,
 44.54417405+112.3087142*I,
 44.99683874+113.7870920*I,
 45.44717089+115.2612977*I,
 45.89522370+116.7314179*I,
 46.34104828+118.1975360*I,
 46.78469382+119.6597323*I,
 47.22620768+121.1180844*I,
 47.66563542+122.5726670*I,
 48.10302096+124.0235525*I,
 48.53840687+125.4708105*I,
 48.97183378+126.9145087*I,
 49.40334123+128.3547122*I,
 49.83296732+129.7914842*I

Zeros of the derivative of $\Gamma(z, 2.5)$ in rectangle with corners (0,0), (50,250).

4.673138861+6.313713520*I,
 6.669823675+9.592500780*I,
 8.213885745+12.46795224*I,
 9.535105445+15.11617279*I,
 10.71753639+17.61144725*I,
 11.80286092+19.99380937*I,
 12.81529823+22.28790950*I,
 13.77038452+24.51027300*I,
 14.67878843+26.67265548*I,

15.54821071+28.78379435*I,
16.38442603+30.85040699*I,
17.19189729+32.87779833*I,
17.97415889+34.87025042*I,
18.73406707+36.83128303*I,
19.47396960+38.76383400*I,
20.19582448+40.67038775*I,
20.90128516+42.55306926*I,
21.59176326+44.41371410*I,
22.26847552+46.25392176*I,
22.93247966+48.07509688*I,
23.58470216+49.87848147*I,
24.22596008+51.66518070*I,
24.85697846+53.43618345*I,
25.47840423+55.19237905*I,
26.09081759+56.93457120*I,
26.69474133+58.66348915*I,
27.29064851+60.37979725*I,
27.87896889+62.08410305*I,
28.46009428+63.77696380*I,
29.03438323+65.45889225*I,
29.60216466+67.13036190*I,
30.16374139+68.79181075*I,
30.71939290+70.44364515*I,
31.26937779+72.08624310*I,
31.81393592+73.71995685*I,
32.35329027+75.34511540*I,
32.88764858+76.96202665*I,
33.41720477+78.57097930*I,
33.94214021+80.17224450*I,
34.46262483+81.76607735*I,
34.97881813+83.35271820*I,
35.49087003+84.93239385*I,
35.99892171+86.50531875*I,
36.50310626+88.07169575*I,
37.00354937+89.63171710*I,
37.50036986+91.18556520*I,
37.99368022+92.73341325*I,
38.48358707+94.27542600*I,
38.97019159+95.81176030*I,
39.45358989+97.34256560*I,
39.93387337+98.86798445*I,

40.41112906+100.3881530*I,
40.88543957+101.9032012*I,
41.35688486+103.4132538*I,
41.82553959+104.9184297*I,
42.29147618+106.4188430*I,
42.75476359+107.9146032*I,
43.21546790+109.4058154*I,
43.67365235+110.8925804*I,
44.12937755+112.3749950*I,
44.58270168+113.8531527*I,
45.03368058+115.3271429*I,
45.48236786+116.7970521*I,
45.92881508+118.2629634*I,
46.37307184+119.7249572*I,
46.81518586+121.1831107*I,
47.25520309+122.6374986*I,
47.69316783+124.0881931*I,
48.12912278+125.5352638*I,
48.56310912+126.9787781*I,
48.99516661+128.4188011*I,
49.42533364+129.8553959*I,
49.85364731+131.2886235*I

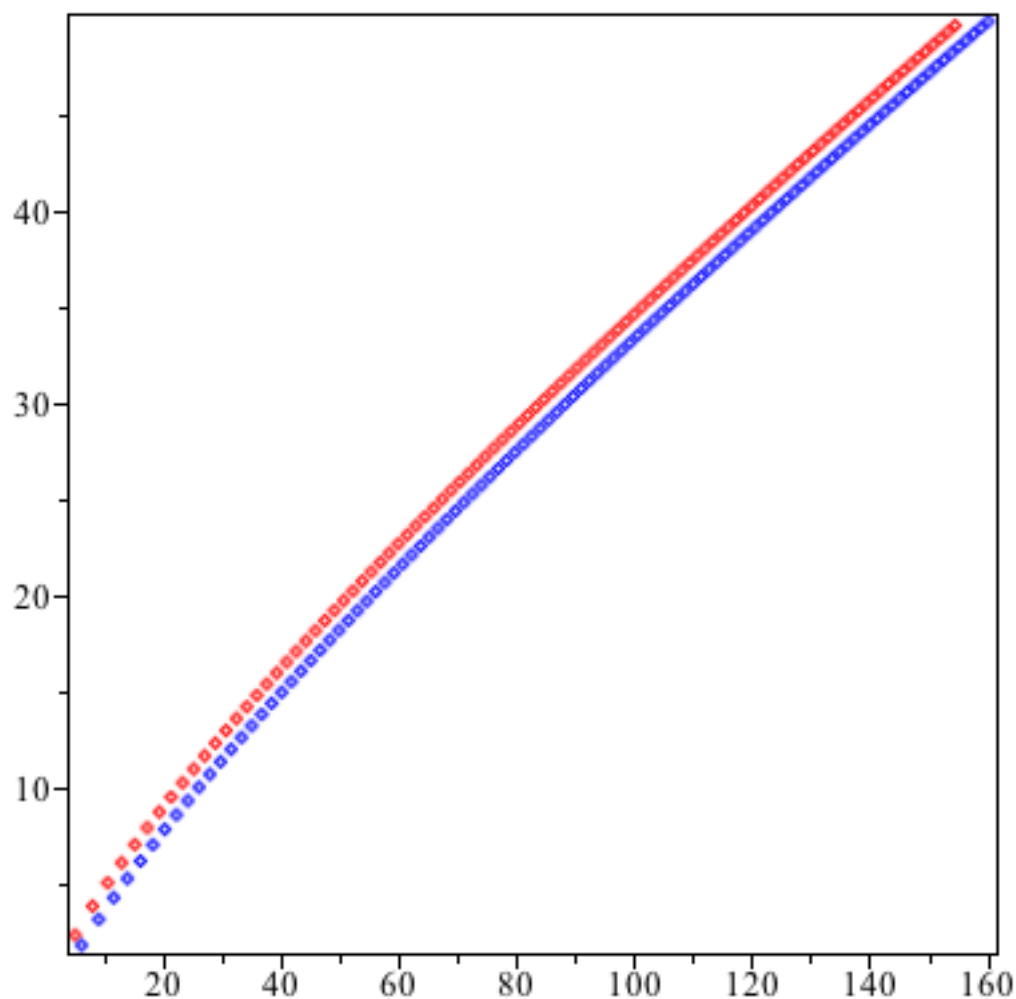


Figure 6: Zeros of $G(z; 1.5, 0.5)$ in red and of its derivative in blue

Zeros of $G(z; 1.5, 0.5)$ in rectangle with corners (0.01,0), (250,50).

4.930509536+2.344806407*I,
 7.887533670+3.853753372*I,
 10.45799459+5.059539400*I,
 12.82456329+6.107220345*I,
 15.05699185+7.054072105*I,
 17.19142967+7.929322735*I,
 19.24969926+8.750257600*I,
 21.24626190+9.528105720*I,
 23.19132932+10.27065308*I,
 25.09245398+10.98356359*I,
 26.95542222+11.67111202*I,
 28.78479237+12.33662021*I,
 30.58423722+12.98273137*I,
 32.35677172+13.61159040*I,
 34.10490997+14.22496688*I,
 35.83077611+14.82434137*I,
 37.53618656+15.41096800*I,
 39.22270938+15.98592028*I,
 40.89171068+16.55012582*I,
 42.54438990+17.10439286*I,
 44.18180755+17.64943082*I,
 45.80490719+18.18586659*I,
 47.41453313+18.71425743*I,
 49.01144474+19.23510146*I,
 50.59632825+19.74884611*I,
 52.16980640+20.25589515*I,
 53.73244660+20.75661448*I,
 55.28476775+21.25133691*I,
 56.82724590+21.74036634*I,
 58.36031930+22.22398107*I,
 59.88439240+22.70243686*I,
 61.39983960+23.17596932*I,
 62.90700830+23.64479618*I,
 64.40622170+24.10911908*I,
 65.89778095+24.56912526*I,
 67.38196751+25.02498893*I,
 68.85904480+25.47687253*I,
 70.32925980+25.92492783*I,
 71.79284455+26.36929691*I,
 73.25001740+26.81011298*I,
 74.70098415+27.24750116*I,

76.14593905+27.68157917*I,
77.58506570+28.11245793*I,
79.01853785+28.54024208*I,
80.44652025+28.96503051*I,
81.86916920+29.38691676*I,
83.28663320+29.80598946*I,
84.69905340+30.22233266*I,
86.10656430+30.63602615*I,
87.50929410+31.04714579*I,
88.90736505+31.45576376*I,
90.30089390+31.86194880*I,
91.68999240+32.26576642*I,
93.07476715+32.66727936*I,
94.45532055+33.06654715*I,
95.83175050+33.46362700*I,
97.20415105+33.85857357*I,
98.57261230+34.25143917*I,
99.93722095+34.64227396*I,
101.2980602+35.03112606*I,
102.6552102+35.41804158*I,
104.0087480+35.80306488*I,
105.3587478+36.18623856*I,
106.7052812+36.56760357*I,
108.0484170+36.94719934*I,
109.3882219+37.32506382*I,
110.7247600+37.70123358*I,
112.0580934+38.07574386*I,
113.3882821+38.44862867*I,
114.7153839+38.81992080*I,
116.0394550+39.18965193*I,
117.3605496+39.55785268*I,
118.6787202+39.92455260*I,
119.9940177+40.28978030*I,
121.3064914+40.65356344*I,
122.6161892+41.01592880*I,
123.9231574+41.37690230*I,
125.2274409+41.73650905*I,
126.5290835+42.09477340*I,
127.8281275+42.45171894*I,
129.1246142+42.80736855*I,
130.4185837+43.16174445*I,
131.7100747+43.51486818*I,

132.9991252+43.86676066*I,
 134.2857719+44.21744224*I,
 135.5700508+44.56693264*I,
 136.8519966+44.91525110*I,
 138.1316434+45.26241624*I,
 139.4090242+45.60844625*I,
 140.6841713+45.95335878*I,
 141.9571160+46.29717104*I,
 143.2278890+46.63989974*I,
 144.4965202+46.98156121*I,
 145.7630387+47.32217132*I,
 147.0274729+47.66174552*I,
 148.2898506+48.00029894*I,
 149.5501988+48.33784625*I,
 150.8085440+48.67440179*I,
 152.0649120+49.00997956*I,
 153.3193277+49.34459283*I,
 154.5718170+49.67825642*I

Zeros of the derivative of $G(z; 1.5, 0.5)$ in rectangle with corners (0.01,0), (250,50).

6.012778145556205933700285+1.816685806631677557038486*I,
 8.946717135741403483682750+3.163596264551669699246458*I,
 11.48273861217396901201504+4.288287138232281657955343*I,
 13.81961172487459047223629+5.284827502352804202776070*I,
 16.02702509250236214206033+6.195739474729819398477650*I,
 18.14016244958958125911735+7.043994725715278238941665*I,
 20.18002565458764171976776+7.843714560006929985126650*I,
 22.16046271081205529371205+8.604334340696817400336300*I,
 24.09123294513378653078772+9.332538027267450402140415*I,
 25.97955121678451514734528+10.03327056397457505768898*I,
 27.83094752559948580622420+10.71031524372258632045882*I,
 29.64978208539358035696880+11.3666451521099833780946*I,
 31.43957196970350304349515+12.00464834253541495880011*I,
 33.20320782872812352982800+12.62627821312947435980360*I,
 34.94310306738257808554544+13.23315743002726922725622*I,
 36.66129972868400579006383+13.82665184597165227733477*I,
 38.35954562099842322936689+14.40792438528901466276114*I,
 40.03935176111626262811608+14.97797516774231794193192*I,
 41.70203598915348154556388+15.53767194440833113428893*I,
 43.34875664754783426445498+16.08777356467023831440936*I,
 44.98053897805553760223254+16.62894833403825461144536*I,
 46.59829608738946808788709+17.16178856232889063952027*I,

48.20284579798027217012371+17.68682222782857500642458*I,
 49.79492433718799601975071+18.20452242815975116625877*I,
 51.37519756645970452357507+18.71531511144842653948631*I,
 52.94427027414996785982150+19.21958545618855566001801*I,
 54.50269392817577390549750+19.71768317829972582969224*I,
 56.05097319181600640806645+20.20992697839793528873712*I,
 57.58957143744156323064610+20.6966082939826233841791*I,
 59.11891544176952015268980+21.17799448515780495417718*I,
 60.63939940755295748879625+21.65433155525388848236023*I,
 62.15138842708114010156785+22.12584648692412309466583*I,
 63.65522148009011362839455+22.59274925827263470987934*I,
 65.15121404096363928529215+23.05523459112255162048668*I,
 66.63966035620018527158970+23.51348347377703164389487*I,
 68.12083544212535867959340+23.96766449292094118713877*I,
 69.59499684406812962736870+24.41793500318093473247642*I,
 71.06238619119056202149377+24.86444215795124008624277*I,
 72.52323057548510767001445+25.30732382113348166387716*I,
 73.97774377884218393306125+25.74670937622752716004104*I,
 75.42612736832238760058393+26.18272044659041718786884*I,
 76.86857167667129039450363+26.61547153853135105447311*I,
 78.30525668255726569667285+27.04507061713872313597724*I,
 79.73635280289000493881690+27.47161962326699189110154*I,
 81.16202160780716123246123+27.89521493888897099436676*I,
 82.58241646743378095841005+28.31594780699722132327388*I,
 83.99768313827191585979835+28.73390471138016168261600*I,
 85.40796029602440739564515+29.14916772087512947664328*I,
 86.81338002076374110656940+29.56181480208842518585317*I,
 88.21406823959689984198260+29.97192010405236966916714*I,
 89.61014513132818180115610+30.37955421784615250390246*I,
 91.00172549706591182919720+30.78478441382814982031835*I,
 92.38891910024101899961130+31.18767485880210894650552*I,
 93.77183097909334422926893+31.58828681515962882080351*I,
 95.15056173432515186221565+31.98667882379967975931986*I,
 96.52520779431223600661370+32.38290687241667186072783*I,
 97.89586165999422134214660+32.77702455056694229030262*I,
 99.26261213133128987611460+33.16908319276543069082570*I,
 100.6255445170096921814080+33.55913201072634761562455*I,
 101.9847408288988736368601+33.94721821574095231254888*I,
 103.3402799626053563944562+34.33338713207972966462572*I,
 104.6922378653296943839238+34.71768230221324895960828*I,
 106.0406876921103357576899+35.10014558456406576494808*I,
 107.3856999514299319034403+35.48081724442971699429344*I,

108. 7273426410636845683998+35. 85973603865289900892256*I,
110. 0656813749641461307519+36. 23693929455823179603157*I,
111. 4007795019011282076618+36. 61246298362467457366060*I,
112. 7326982165078642263918+36. 98634179031787470684666*I,
114. 0614966633243054643306+37. 35860917646681739058268*I,
115. 3872320343745362609064+37. 72929744153350616287592*I,
116. 7099596607670172345397+38. 09843777909253132822591*I,
118. 0297330987630489620383+38. 46606032980882993763946*I,
119. 3466042107199210442964+38. 83219423117632022102620*I,
120. 6606232412801739613588+39. 19686766425706818376092*I,
121. 9718388891468174668741+39. 56010789763992011072419*I,
123. 2802983747558374165954+39. 92194132881885446352634*I,
124. 5860475041315475437564+40. 2823935231744441662660*I,
125. 8891307291870089539546+40. 64148925072657988334860*I,
127. 1895912047105883271772+40. 99925252081280101768149*I,
128. 4874708422605268615059+41. 35570661483409024671656*I,
129. 7828103611719433766764+41. 71087411719862132588227*I,
131. 0756493368648174635329+42. 06477694458365186708560*I,
132. 3660262466270331881203+42. 41743637362636414718147*I,
133. 6539785130333695089160+42. 76887306714591364831817*I,
134. 9395425451492747337346+43. 11910709899115212346368*I,
136. 2227537776572472470988+43. 46815797760137766776976*I,
137. 5036467080335636803005+43. 81604466836096207853364*I,
138. 7822549318938596287572+44. 16278561482275662381254*I,
140. 0586111766175973045861+44. 50839875886972843955588*I,
141. 3327473333536778245351+44. 85290155987928393529731*I,
142. 6046944875023092187281+45. 19631101295015053414879*I,
143. 8744829477616672810526+45. 53864366624747589393240*I,
145. 1421422738218334460280+45. 87991563751793041415677*I,
146. 4077013027829155074452+46. 22014262982303372863172*I,
147. 6711881743691113230118+46. 55933994653564147490647*I,
148. 9326303550057249047998+46. 89752250564150010261139*I,
150. 1920546608217543627705+47. 23470485338498244557597*I,
151. 4494872796366112018112+47. 57090117729553501840546*I,
152. 7049537919857725509198+47. 90612531862898122710546*I,
153. 9584791912366867268000+48. 24039078425561636054924*I,
155. 2100879028430251548646+48. 57371075802498536516622*I,
156. 4598038027823792518021+48. 90609811163533940413076*I,
157. 7076502352197204772291+49. 23756541503400972209018*I,
158. 9536500294363581580314+49. 56812494637330616090333*I,
160. 1978255160617271879464+49. 89778870154503259837316*I

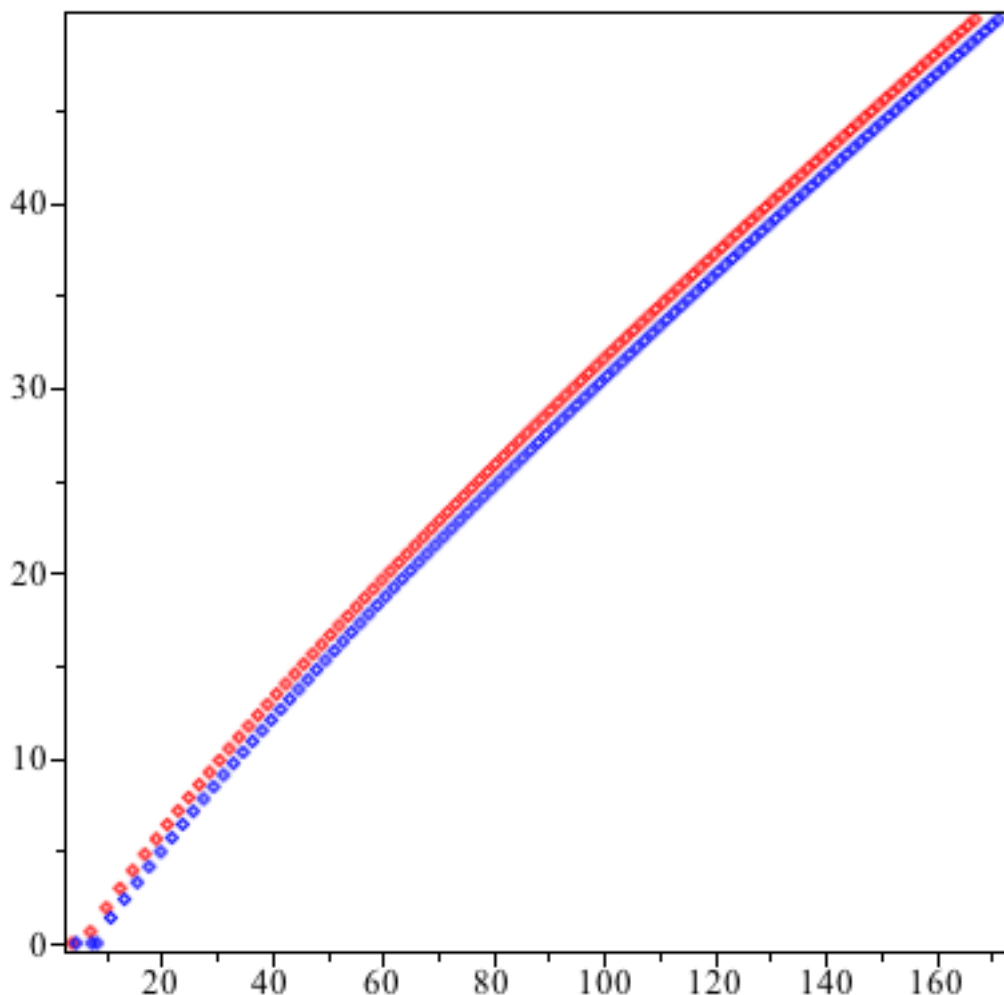


Figure 7: Zeros of $G(z; 1.5, 1.5)$ in red and of its derivative in blue

Zeros of $G(z; 1.5, 1.5)$ in rectangle with corners (0.01,0), (250,50).

3.937905687,
 7.251513627+.6107439837*I,
 10.12360981+1.903711076*I,
 12.59124934+2.964286416*I,
 14.87966733+3.919174854*I,
 17.04985809+4.800045080*I,
 19.13298468+5.625227920*I,
 21.14784064+6.406456279*I,
 23.10693326+7.151792462*I,
 25.01914884+7.867066170*I,
 26.89110279+8.556659971*I,
 28.72789672+9.223965825*I,
 30.53357592+9.871677515*I,
 32.31141650+10.50197919*I,
 34.06412296+11.11666447*I,
 35.79396034+11.71723378*I,
 37.50285552+12.30496601*I,
 39.19245796+12.88093626*I,
 40.86419832+13.44609427*I,
 42.51932997+14.00124869*I,
 44.15895444+14.54711765*I,
 45.78405010+15.08433859*I,
 47.39548780+15.61347150*I,
 48.99405218+16.13501372*I,
 50.58045060+16.64942390*I,
 52.15531945+17.15710595*I,
 53.71923580+17.65842243*I,
 55.27274135+18.15371994*I,
 56.81631710+18.64329210*I,
 58.35041105+19.12743180*I,
 59.87543670+19.60639366*I,
 61.39176620+20.08042226*I,
 62.89977160+20.54972471*I,
 64.39974665+21.01448388*I,
 65.89203190+21.47492077*I,
 67.37690485+21.93120568*I,
 68.85461480+22.38349109*I,
 70.32544330+22.83194031*I,
 71.78959795+23.27668059*I,
 73.24731060+23.71787799*I,
 74.69879350+24.15561319*I,

76.14424355+24.59004556*I,
77.58382005+25.02125740*I,
79.01771980+25.44936066*I,
80.44612175+25.87445412*I,
81.86918835+26.29667290*I,
83.28702460+26.71602009*I,
84.69979655+27.13264381*I,
86.10764730+27.54666567*I,
87.51071435+27.95804704*I,
88.90909710+28.36695130*I,
90.30292400+28.77339900*I,
91.69230585+29.17745205*I,
93.07736820+29.57923665*I,
94.45817960+29.97874025*I,
95.83488500+30.37607838*I,
97.20750330+30.77120792*I,
98.57619880+31.16435306*I,
99.94104950+31.55541870*I,
101.3020818+31.94447933*I,
102.6594611+32.33164194*I,
104.0131896+32.71684608*I,
105.3633836+33.10022927*I,
106.7101026+33.48179934*I,
108.0534227+33.86157431*I,
109.3934006+34.23971774*I,
110.7301175+34.61605250*I,
112.0636115+34.99077168*I,
113.3939414+35.36381285*I,
114.7212276+35.73529304*I,
116.0454060+36.10514746*I,
117.3666622+36.47358976*I,
118.6849925+36.84041339*I,
120.0004036+37.20590617*I,
121.3129930+37.56980410*I,
122.6228475+37.93230992*I,
123.9299068+38.29342338*I,
125.2342994+38.65318830*I,
126.5360900+39.01167600*I,
127.8352154+39.36874859*I,
129.1318420+39.72450698*I,
130.4258786+40.07901733*I,
131.7174605+40.43236320*I,

133.0066207+40.78437228*I,
 134.2933320+41.13518979*I,
 135.5777499+41.48485416*I,
 136.8598452+41.83351800*I,
 138.1395566+42.18072661*I,
 139.4169953+42.52690826*I,
 140.6921776+42.87187780*I,
 141.9652842+43.21583448*I,
 143.2360706+43.55864397*I,
 144.5048026+43.90042138*I,
 145.7714049+44.24125044*I,
 147.0358727+44.58076756*I,
 148.2983600+44.91953434*I,
 149.5587354+45.25722820*I,
 150.8171880+45.59401438*I,
 152.0736012+45.92968392*I,
 153.3280566+46.26424587*I,
 154.5806022+46.59795682*I,
 155.8313212+46.93092457*I,
 157.0800599+47.26281420*I,
 158.3269492+47.59376888*I,
 159.5719638+47.92385924*I,
 160.8152711+48.25319042*I,
 162.0566793+48.58140666*I,
 163.2965010+48.90895708*I,
 164.5343684+49.23573476*I,
 165.7705745+49.56130794*I,
 167.0051230+49.88623883*I

Zeros of the derivative of $G(z; 1.5, 1.5)$ in rectangle with corners (0.01,0), (250,50).

4.667700946,
 7.483808310,
 8.407400255,
 10.91195567+1.365745584*I,
 13.39023297+2.369900146*I,
 15.67830509+3.283486490*I,
 17.84460858+4.132243178*I,
 19.92240068+4.931563363*I,
 21.93137142+5.691387905*I,
 23.88444642+6.418626360*I,
 25.79071631+7.118334843*I,
 27.65689195+7.794350635*I,

29.48811465+8.449671525*I,
 31.28846455+9.086710847*I,
 33.06119737+9.707415100*I,
 34.80902847+10.31341524*I,
 36.53420862+10.90607470*I,
 38.23865246+11.48655147*I,
 39.92399502+12.05585095*I,
 41.59165762+12.61482951*I,
 43.24285997+13.16425792*I,
 44.87876304+13.70478333*I,
 46.50024609+14.23701387*I,
 48.10821144+14.76146515*I,
 49.70345400+15.27859999*I,
 51.28665749551745816453620+15.78886530298144847001386*I,
 52.85843489316570252453195+16.29262608568675623332408*I,
 54.41937302709357276288645+16.79023592374016476039430*I,
 55.96999636550351471433125+17.28201206513609720331654*I,
 57.51078540445273716556180+17.76824461535208046389930*I,
 59.04218180422940486964715+18.24919971288210636996778*I,
 60.56459276756654264770010+18.72512224012151522657222*I,
 62.07839479345482148735440+19.19623815035266164680648*I,
 63.58393691310301659390635+19.66275647546503846254189*I,
 65.08154349360848788736905+20.12487106653535681211041*I,
 66.57151667856676391428435+20.58276210960225841068042*I,
 68.05413852202901288926790+21.03659745124565496942059*I,
 69.52967286207311872032890+21.48653376244079979857754*I,
 70.99836697216934495860265+21.93271756424289421349942*I,
 72.46045302203242306391930+22.37528613489885475646052*I,
 73.91614937440922964851000+22.81436831477345338392334*I,
 75.36566173998939756635280+23.25008522286021892438254*I,
 76.80918420914152441855280+23.68255089650206184082066*I,
 78.24690017631268928664495+24.11187286417844492798996*I,
 79.67898317056126832629245+24.53815265975149955205757*I,
 81.10559760372658512763050+24.96148628534490178606365*I,
 82.52689944609807977523090+25.38196462901076702660434*I,
 83.94303683807141669729565+25.79967384248483255357200*I,
 85.35415064512139938052060+26.21469568360959263115854*I,
 86.76037496244331840906020+26.62710782739535323311590*I,
 88.16183757478446601914030+27.03698414917140270717512*I,
 89.55866037628091785320460+27.44439498283823259436700*I,
 90.95095975451088684917575+27.84940735685440845492727*I,
 92.33884694245829266824240+28.25208521026797361551611*I,

93.72242834163494443501790+28.65248959082368461694440*I,
95.10180581922559087064530+29.05067883693691587173812*I,
96.47707698178768207744800+29.44670874511691889123698*I,
97.84833542774922483410580+29.84063272424143906893213*I,
99.21567098069710279790330+30.23250193792743798662312*I,
100.5791699052292368493373+30.62236543610545324018698*I,
101.9389151069524114958910+31.01027027678510172023570*I,
103.2949863180396417534482+31.39626163889399262443442*I,
104.6474602696133475326060+31.78038292697982967484910*I,
105.9964108520905803911204+32.16267586848402235032568*I,
107.3419092645117645747880+32.54318060422322491295106*I,
108.6840241537728699467173+32.92193577265162645152508*I,
110.0228217445909180190536+33.29897858842045299724020*I,
111.3583659609527673087397+33.67434491570109433999983*I,
112.6907185397259700957578+34.04806933669374275803267*I,
114.0199391370470533127284+34.42018521570374689380691*I,
115.3460854280459137867212+34.79072475913245268605817*I,
116.6692132004143204220631+35.15971907169761466895364*I,
117.9893764422810787506815+35.52719820917007283831532*I,
119.3066274248156241802010+35.89319122788791774387714*I,
120.6210167799451355703192+36.25772623128647447435085*I,
121.9325935735372347245965+36.62083041366183194759131*I,
123.2414053743705523805812+36.98253010136707141929095*I,
124.5474983191885402819956+37.34285079162358300882897*I,
125.8509171741075782752087+37.70181718911470422221956*I,
127.1517053926283891958323+38.05945324051519672215169*I,
128.4499051704797896202648+38.41578216709764414816102*I,
129.7455574975056566776468+38.77082649554556996817593*I,
131.0387022067894903838234+39.12460808709282090510301*I,
132.3293780211959293325644+39.47714816509943302049992*I,
133.6176225974948860478762+39.82846734116570041596838*I,
134.9034725682214744313096+40.17858563987841771745430*I,
136.1869635814134877205135+40.52752252227619307214798*I,
137.4681303383577463633782+40.87529690811426247477382*I,
138.7470066294670773383916+41.22192719700332017862231*I,
140.0236253684009262753468+41.56743128849146121817402*I,
141.2980186245345662004833+41.9118266011533637432221*I,
142.5702176538744848195394+42.25513009074627903698267*I,
143.8402529285107458208980+42.59735826748820785182481*I,
145.1081541646908746760877+42.93852721250978950288329*I,
146.3739503495940670404668+43.27865259352788428821295*I,
147.6376697668792147456766+43.61774967978556312975885*I,

148.8993400210753505940000+43.95583335630020603850000*I,
150.1589880608785934231248+44.29291813745863085439712*I,
151.4166402014154970096470+44.62901817999560569560898*I,
152.6723221455288409827468+44.96414729538972435525843*I,
153.9260590041383230100630+45.29831896170842719496580*I,
155.1778753157252949249296+45.63154633493191587742303*I,
156.4277950649876096349376+45.96384225978382519807672*I,
157.6758417007077909635500+46.29521928009476681748100*I,
158.9220381528750869563046+46.62568964872323698477350*I,
160.1664068490995025013470+46.95526533705687297550100*I,
161.4089697303536143919008+47.28395804411564192599530*I,
162.6497482660758378422895+47.61177920527724245180516*I,
163.8887634686668254156315+47.93874000064378627306224*I,
165.1260359074088261245520+48.26485136306769710025070*I,
166.3615857218361039395145+48.59012398585371068732322*I,
167.5954326345829013448354+48.91456833015287756228378*I,
168.8275959637339267166710+49.23819463206355295688505*I,
170.0580946347009356210960+49.56101290945350215429520*I,
171.2869471916476591982430+49.88303296851644914829712*I

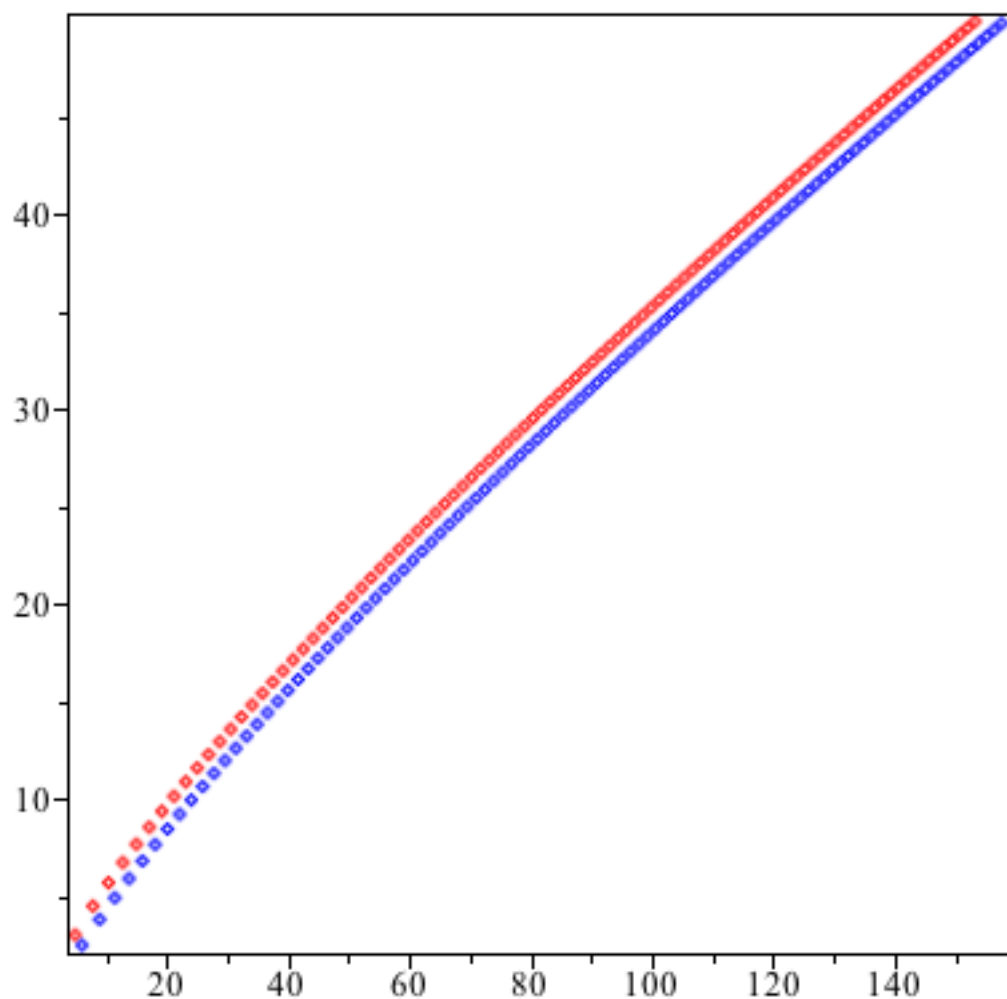


Figure 8: Zeros of $G(z; 1.5, 0)$ in red and of its derivative in blue

Zeros of $G(z; 1.5, 0)$ in rectangle with corners (0.01,0), (250,50).

4.918293784+3.035804313*I,
 7.855077370+4.521631898*I,
 10.42198413+5.713456405*I,
 12.78793500+6.752038915*I,
 15.02057324+7.692317805*I,
 17.15549805+8.562501560*I,
 19.21434510+9.379356290*I,
 21.21150298+10.15381474*I,
 23.15715338+10.89347941*I,
 25.05883645+11.60389345*I,
 26.92233411+12.28924827*I,
 28.75220392+12.95280594*I,
 30.55211959+13.59716552*I,
 32.32509771+14.22443843*I,
 34.07365422+14.83636825*I,
 35.79991540+15.43441520*I,
 37.50569934+16.01981687*I,
 39.19257591+16.59363346*I,
 40.86191282+17.15678160*I,
 42.51491098+17.71006039*I,
 44.15263221+18.25417156*I,
 45.77602127+18.78973548*I,
 47.38592353+19.31730387*I,
 48.98309935+19.83737005*I,
 50.56823580+20.35037729*I,
 52.14195645+20.85672577*I,
 53.70482945+21.35677819*I,
 55.25737430+21.85086461*I,
 56.80006770+22.33928643*I,
 58.33334835+22.82231978*I,
 59.85762130+23.30021842*I,
 61.37326135+23.77321625*I,
 62.88061630+24.24152940*I,
 64.38000975+24.70535809*I,
 65.87174325+25.16488828*I,
 67.35609855+25.62029299*I,
 68.83333930+26.07173359*I,
 70.30371280+26.51936095*I,
 71.76745140+26.96331618*I,
 73.22477365+27.40373170*I,
 74.67588560+27.84073190*I,

76.12098165+28.27443380*I,
77.56024560+28.70494767*I,
78.99385145+29.13237758*I,
80.42196400+29.55682187*I,
81.84473980+29.97837358*I,
83.26232740+30.39712081*I,
84.67486825+30.81314731*I,
86.08249685+31.22653234*I,
87.48534155+31.63735142*I,
88.88352475+32.04567636*I,
90.27716325+32.45157560*I,
91.66636890+32.85511436*I,
93.05124850+33.25635491*I,
94.43190445+33.65535672*I,
95.80843475+34.05217664*I,
97.18093350+34.44686910*I,
98.54949095+34.83948620*I,
99.91419380+35.23007788*I,
101.2751255+35.61869198*I,
102.6323660+36.00537451*I,
103.9859925+36.39016961*I,
105.3360793+36.77311970*I,
106.6826981+37.15426557*I,
108.0259177+37.53364649*I,
109.3658048+37.91130028*I,
110.7024237+38.28726334*I,
112.0358364+38.66157079*I,
113.3661030+39.03425650*I,
114.6932814+39.40535317*I,
116.0174277+39.77489234*I,
117.3385963+40.14290450*I,
118.6568396+40.50941912*I,
119.9722086+40.87446470*I,
121.2847527+41.23806877*I,
122.5945197+41.60025811*I,
123.9015560+41.96105847*I,
125.2059066+42.32049490*I,
126.5076152+42.67859166*I,
127.8067242+43.03537226*I,
129.1032750+43.39085953*I,
130.3973074+43.74507558*I,
131.6888605+44.09804192*I,

132.9779722+44.44977938*I,
 134.2646792+44.80030820*I,
 135.5490176+45.14964816*I,
 136.8310220+45.49781836*I,
 138.1107266+45.84483738*I,
 139.3881644+46.19072333*I,
 140.6633676+46.53549383*I,
 141.9363678+46.87916602*I,
 143.2071955+47.22175660*I,
 144.4758806+47.56328180*I,
 145.7424523+47.90375750*I,
 147.0069390+48.24319908*I,
 148.2693686+48.58162159*I,
 149.5297680+48.91903973*I,
 150.7881637+49.25546777*I,
 152.0445816+49.59091964*I,
 153.2990470+49.92540899*I

Zeros of the derivative of $G(z; 1.5, 0)$ in rectangle with corners (0.01,0), (250,50).

6.055175040+2.509891054*I,
 8.941093605+3.831161188*I,
 11.46529262+4.941189375*I,
 13.79725980+5.928524430*I,
 16.00222937+6.832893300*I,
 18.11404312+7.676147400*I,
 20.15316722+8.471859295*I,
 22.13319801+9.229158615*I,
 24.06376327+9.954542980*I,
 25.95200354+10.65283606*I,
 27.80340436+11.32773810*I,
 29.62229812+11.98216304*I,
 31.41218386+12.61845545*I,
 33.17594023+13.23853581*I,
 34.91597245+13.84400140*I,
 36.63431684+14.43619804*I,
 38.33271724+15.01627269*I,
 40.01268180+15.58521243*I,
 41.67552630+16.14387433*I,
 43.32240764+16.69300834*I,
 44.95434998+17.23327532*I,
 46.57226566+17.76526120*I,
 48.17697191+18.28948864*I,

49.76920466+18.80642598*I,
51.34962947+19.31649513*I,
52.91885085+19.82007802*I,
54.47742030+20.31752098*I,
56.02584230+20.80914012*I,
57.56458030+21.29522450*I,
59.09406100+21.77603930*I,
60.61467870+22.25182864*I,
62.12679850+22.72281782*I,
63.63075950+23.18921523*I,
65.12687710+23.65121428*I,
66.61544565+24.10899466*I,
68.09674040+24.56272383*I,
69.57101880+25.01255810*I,
71.03852255+25.45864368*I,
72.49947890+25.90111761*I,
73.95410153+26.34010846*I,
75.40259250+26.77573704*I,
76.84514185+27.20811730*I,
78.28192965+27.63735652*I,
79.71312650+28.06355612*I,
81.13889390+28.48681190*I,
82.55938540+28.90721465*I,
83.97474680+29.32485036*I,
85.38511685+29.73980071*I,
86.79062760+30.15214324*I,
88.19140520+30.56195171*I,
89.58756970+30.96929642*I,
90.97923610+31.37424430*I,
92.36651410+31.77685914*I,
93.74950880+32.17720202*I,
95.12832095+32.57533115*I,
96.50304690+32.97130226*I,
97.87377925+33.36516875*I,
99.24060690+33.75698166*I,
100.6036151+34.14679006*I,
101.9628859+34.53464088*I,
103.3184983+34.92057934*I,
104.6705283+35.30464877*I,
106.0190490+35.68689078*I,
107.3641310+36.06734563*I,
108.7058422+36.44605182*I,

110.0442484+36.82304652*I,
111.3794130+37.19836562*I,
112.7113972+37.57204363*I,
114.0402600+37.94411392*I,
115.3660594+38.31460903*I,
116.6888488+38.68355887*I,
118.0086840+39.05099460*I,
119.3256157+39.41694492*I,
120.6396942+39.78143798*I,
121.9509690+40.14450082*I,
123.2594866+40.50615982*I,
124.5652930+40.86644042*I,
125.8684327+41.22536745*I,
127.1689488+41.58296456*I,
128.4668834+41.93925521*I,
129.7622771+42.29426182*I,
131.0551694+42.64800618*I,
132.3455992+43.00050960*I,
133.6336035+43.35179254*I,
134.9192188+43.70187516*I,
136.2024809+44.05077677*I,
137.4834238+44.39851648*I,
138.7620815+44.74511247*I,
140.0384865+45.09058274*I,
141.3126710+45.43494463*I,
142.5846657+45.77821518*I,
143.8545012+46.12041074*I,
145.1222070+46.46154758*I,
146.3878120+46.80164116*I,
147.6513442+47.14070692*I,
148.9128312+47.47875958*I,
150.1722998+47.81581368*I,
151.4297764+48.15188350*I,
152.6852862+48.48698274*I,
153.9388544+48.82112481*I,
155.1905054+49.15432294*I,
156.4402632+49.48658992*I,
157.6881510+49.81793834*I

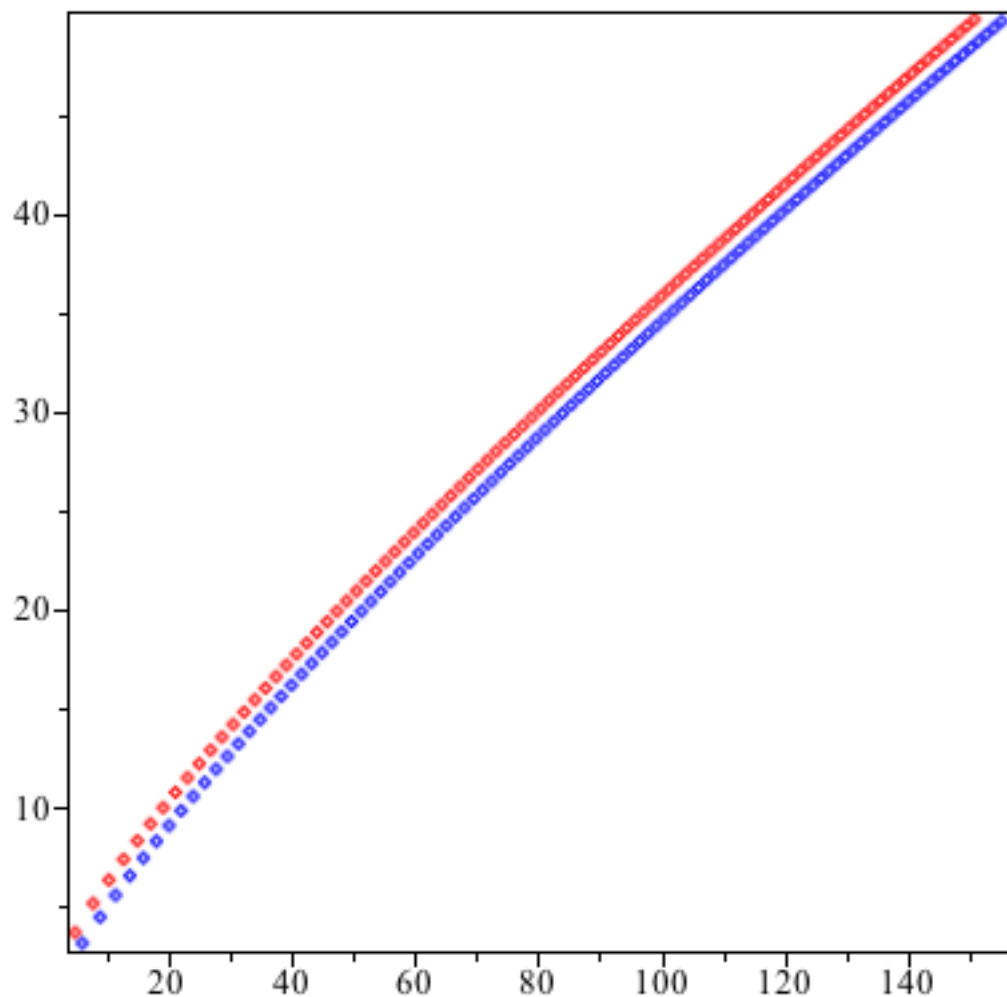


Figure 9: Zeros of $G(z; 1.5, -0.5)$ in red and of its derivative in blue

Zeros of $G(z; 1.5, -0.5)$ in rectangle with corners (0.01,0), (250,50).

4.918571547248116910117103+3.654246682837711926781984*I,
 7.841896814851529791354100+5.133090427245470509613270*I,
 10.40436799197687719272643+6.318286124641223022033070*I,
 12.76846632387278753130505+7.351875263082797880771915*I,
 15.00024993276077965837001+8.288285541871233174044485*I,
 17.13478234398162827614478+9.155362130443096774080525*I,
 19.19347599671980026620459+9.969646596285818041293380*I,
 21.19061298518832014703360+10.74192894200378114915656*I,
 23.13631921629433654103878+11.47971689491351098863834*I,
 25.03810359424844276724184+12.18848807848128992246964*I,
 26.90172962761340986521853+12.87238700647490326901014*I,
 28.73174362271471160075646+13.53464119665221361804970*I,
 30.53181220599742547077000+14.17782357344041854205977*I,
 32.30494741769529281972066+14.80402539148552197593028*I,
 34.05366220130566089322250+15.41497439967318570792248*I,
 35.78008102725542222794108+16.01211807757056762187121*I,
 37.48602059705773897407634+16.59668380397990930580197*I,
 39.17305000730512853395031+17.16972333013752552123057*I,
 40.84253645399869111189665+17.73214629550954965502210*I,
 42.49568053194073053592385+18.28474592004035246371258*I,
 44.13354390073242894703790+18.82821899868761900724375*I,
 45.75707125366195385569459+19.36318167281124386090557*I,
 47.36710796880176718860344+19.89018202174441988102998*I,
 48.96441444215488402663527+20.40971022600187072796210*I,
 50.54967785+20.92220685*I,
 52.12352180+21.42806967*I,
 53.68651460+21.92765929*I,
 55.23917590+22.42130392*I,
 56.78198245+22.90930331*I,
 58.31537310+23.39193213*I,
 59.83975305+23.86944282*I,
 61.35549715+24.34206811*I,
 62.86295345+24.81002306*I,
 64.36244550+25.27350695*I,
 65.85427505+25.73270484*I,
 67.33872395+26.18778898*I,
 68.81605590+26.63892003*I,
 70.28651840+27.08624815*I,
 71.75034380+27.52991390*I,
 73.20775075+27.97004914*I,
 74.65894535+28.40677772*I,

76.10412215+28.84021622*I,
77.54346500+29.27047446*I,
78.97714790+29.69765612*I,
80.40533585+30.12185914*I,
81.82818540+30.54317624*I,
83.24584515+30.96169524*I,
84.65845655+31.37749945*I,
86.06615425+31.79066798*I,
87.46906665+32.20127605*I,
88.86731615+32.60939523*I,
90.26101965+33.01509372*I,
91.65028895+33.41843652*I,
93.03523100+33.81948572*I,
94.41594815+34.21830057*I,
95.79253855+34.61493778*I,
97.16509625+35.00945158*I,
98.53371155+35.40189391*I,
99.89847125+35.79231455*I,
101.2594587+36.18076126*I,
102.6167540+36.56727986*I,
103.9704343+36.95191436*I,
105.3205741+37.33470708*I,
106.6672448+37.71569870*I,
108.0105155+38.09492836*I,
109.3504529+38.47243379*I,
110.6871213+38.84825128*I,
112.0205827+39.22241588*I,
113.3508971+39.59496136*I,
114.6781226+39.96592031*I,
116.0023153+40.33532422*I,
117.3235295+40.70320350*I,
118.6418178+41.06958753*I,
119.9572311+41.43450475*I,
121.2698188+41.79798266*I,
122.5796288+42.16004786*I,
123.8867074+42.52072616*I,
125.1910997+42.88004248*I,
126.4928494+43.23802106*I,
127.7919990+43.59468536*I,
129.0885898+43.95005812*I,
130.3826616+44.30416144*I,
131.6742536+44.65701674*I,

132.9634036+45.00864484*I,
 134.2501486+45.35906596*I,
 135.5345242+45.70829974*I,
 136.8165655+46.05636529*I,
 138.0963064+46.40328118*I,
 139.3737801+46.74906546*I,
 140.6490188+47.09373572*I,
 141.9220539+47.43730905*I,
 143.1929162+47.77980212*I,
 144.4616355+48.12123116*I,
 145.7282409+48.46161195*I,
 146.9927609+48.80095990*I,
 148.2552233+49.13929000*I,
 149.5156552+49.47661693*I,
 150.7740831+49.81295490*I

Zeros of the derivative of $G(z; 1.5, -0.5)$ in rectangle with corners (0.01,0), (250,50).

6.094213420704737735160435+3.118635463969787968256242*I,
 8.950657216792105729802910+4.438288561925345058770253*I,
 11.46399701610219246892422+5.543072863694853382048090*I,
 13.79059322992510867867950+6.526108066952662232230220*I,
 15.99246764875403998977712+7.427035193497844865119147*I,
 18.10233070309795658777548+8.267473956570995408589015*I,
 20.14015214856850392815111+9.060828510747485526047075*I,
 22.11927817696123900198654+9.816114185779634445462570*I,
 24.04919763760708329105230+10.53974994464486469608213*I,
 25.93696829806244974106394+11.23650378355510073652583*I,
 27.78802359874493802014878+11.91003546491769850640282*I,
 29.60666170121163688980104+12.56322869847016121394526*I,
 31.39635834928212988690400+13.19840495088903534545570*I,
 33.15997584631224973820438+13.81746678462666061330290*I,
 34.89990767508638745084836+14.42199724397164396031896*I,
 36.61818158756635006254220+15.01333074718589225104752*I,
 38.31653496110459571463742+15.59260489314722406718021*I,
 39.99647108571370180336569+16.16079912147832044020946*I,
 41.65930200543500529248502+16.71876409458346638173386*I,
 43.30618166810047501435802+17.26724439102014662324060*I,
 44.93813195312387680434821+17.80689628552410475493382*I,
 46.55606337508208832123776+18.33830185894264134291646*I,
 48.16079174557670853035108+18.86198032535562960635988*I,
 49.75305172437881657633094+19.37839722046095209585618*I,
 51.33350794640319135224965+19.88797192598645644159200*I,

52.90276423804167192457895+20.39108388499142799076124*I,
54.46137131197367873753455+20.88807777669027398436400*I,
56.00983323880873983918065+21.37926785653231767182260*I,
57.54861292681922320266430+21.86494162079300869149068*I,
59.07813679081412574250295+22.34536292017477176607155*I,
60.59879875321231354154080+22.82077462063621771537172*I,
62.11096369132495700972645+23.29140088959499159674900*I,
63.61497042243213484308305+23.75744917017049934454889*I,
65.11113430077180933779120+24.21911189409069334505660*I,
66.59974948684049578498745+24.67656797444128366744642*I,
68.08109093854543196575480+25.12998411196901163966858*I,
69.55541616508890849061105+25.57951594270542320795976*I,
71.02296677751327727314270+26.02530904991153087234714*I,
72.48396986421736716830555+26.46749985949841588648395*I,
73.93863921518779412209350+26.90621643495751346557456*I,
75.38717641495411243581710+27.34157918528619686571333*I,
76.82977182120646197962930+27.77370149730279237453750*I,
78.26660544347715413353955+28.20269030201965799231440*I,
79.69784773418069206059035+28.62864658331245533614836*I,
81.12366030254894277378650+29.05166583593230440559320*I,
82.54419656052522304936475+29.47183847891080348117386*I,
83.95960230844158293132510+29.88925022957058823929238*I,
85.37001626725637662244355+30.30398244264788208992936*I,
86.77557056324108355966650+30.7161124184355010945247*I,
88.17639117024936481182615+31.12571368334705573225535*I,
89.57259831405559677611245+31.53285624586842560212342*I,
90.96430684269669366919500+31.93760683049459669403618*I,
92.35162656627519328817460+32.34002909192829729814498*I,
93.73466256927119834973585+32.74018381154561943358202*I,
95.11351549805578852031535+33.13812907789582824422659*I,
96.48828182599059398165215+33.53392045279804158425590*I,
97.85905409823038377505310+33.92761112441946708437236*I,
99.22592115811194053194850+34.31925204856494807192626*I,
100.5889683568082708777823+34.70889207927232559249733*I,
101.9482777477482122568782+35.09657808968977950721361*I,
103.3039282671442554797477+35.48235508410751075862063*I,
104.6559959018329523161425+35.86626630192487452230392*I,
106.0045538455101062320803+36.24835331425367640091820*I,
107.3496726443349097402710+36.62865611378735907061308*I,
108.6914203327814626162952+37.00721319850300382023397*I,
110.0298625605311119794832+37.38406164970739654255397*I,
111.3650627111234494255844+37.75923720488895677094364*I,

112.6970820130164204974938+38.13277432579332352843362*I,
114.0259796436458449533308+38.50470626210116243292562*I,
115.3518128270208447260700+38.87506511105172509717479*I,
116.6746369253434775288100+39.24388187332435236218236*I,
117.9945055250976235894376+39.61118650546203154443670*I,
119.3114705180133012488920+39.97700796909591561064855*I,
120.6255821772775968871211+40.34137427720705862820947*I,
121.9368892293318510336212+40.70431253764122842938873*I,
123.2454389215662646182772+41.06584899407427168605920*I,
124.5512770861973427333686+41.42600906460890717396285*I,
125.8544482005902839630885+41.78481737816881551309914*I,
127.1549954442672922683589+42.14229780884230707054467*I,
128.4529607528236070271750+42.49847350831553326868378*I,
129.7483848689556131011086+42.85336693652402718681125*I,
131.0413073907895278736779+43.20699989064119941307724*I,
132.3317668176847074950713+43.55939353251317038874194*I,
133.6198005936724292295597+43.91056841464089855350774*I,
134.9054451486789655719239+44.26054450480288233578189*I,
136.1887359376707571027918+44.60934120940470038187267*I,
137.4697074778494153674880+44.95697739563524329789224*I,
138.7483933840150554931435+45.30347141250362351938604*I,
140.0248264022079912928602+45.64884111082537584828786*I,
141.2990384417310520312408+45.99310386222163329483026*I,
142.5710606056476359805463+46.33627657719043956142142*I,
143.8409232198440440382030+46.67837572230520352018633*I,
145.1086558607385854515270+47.01941733659147888243133*I,
146.3742873817143707008546+47.35941704712973383141666*I,
147.6378459383475620102410+47.69839008392853358956493*I,
148.8993590124981020565462+48.03635129410956929423598*I,
150.1588534353255521555639+48.37331515544320712686824*I,
151.4163554092886117031059+48.70929578927068247452115*I,
152.6718905291831330463474+49.04430697284670700311222*I,
153.9254838022699649798104+49.37836215113407559611896*I,
155.1771596675407307728632+49.71147444807984039886036*I

Table 3: Interlacing of zeros of $G(z; 1.5, b)$ and of its derivative

b	Real Parts	Imaginary Parts	Modulus
-5	Yes	No	Yes
-4.5	Yes	No	Yes
-4	Yes	No	Yes
-3.5	Yes	No	Yes
-3	Yes	No	Yes
-2.5	Yes	No	Yes
-2	Yes	No	Yes
-1.5	Yes	No	Yes
-1	Yes	No	Yes
-0.5	Yes	No	Yes
0	Yes	No	Yes
0.5	Yes	No	Yes
1	Yes	No	Yes
1.5	No	No	No
2	Yes	No	Yes
2.5	Yes	No	Yes
3	No	No	No
3.5	Yes	No	Yes
4	—	—	—
4.5	No	No	No
5	No	No	No
5.5	No	No	No
6	—	—	—
6.5	—	—	—
7	No	No	No

Table 4: Interlacing of zeros of $G(z; 2, b)$ and of its derivative

b	Real Parts	Imaginary Parts	Modulus
-5	Yes	No	Yes
-4.5	Yes	No	Yes
-4	Yes	No	Yes
-3.5	Yes	No	Yes
-3	Yes	No	Yes
-2.5	Yes	No	Yes
-2	Yes	No	Yes
-1.5	Yes	No	Yes
-1	Yes	No	Yes
-0.5	Yes	No	Yes
0	Yes	No	Yes
0.5	Yes	No	Yes
1	Yes	No	Yes
1.5	Yes	No	Yes
2	Yes	No	Yes
2.5	Yes	No	Yes
3	Yes	No	Yes
3.5	No	No	No
4	No	No	No
4.5	Yes	No	Yes
5	Yes	No	Yes
5.5	No	No	No
6	No	No	No
6.5	Yes	No	Yes
7	No	No	No

Table 5: Interlacing of zeros of $G(z; 2.5, b)$ and of its derivative

b	Real Parts	Imaginary Parts	Modulus
0	Yes	No	Yes
0.5	Yes	No	Yes
1	Yes	No	Yes
1.5	Yes	No	Yes
2	Yes	No	Yes
2.5	Yes	No	Yes
3	Yes	No	Yes
3.5	Yes	No	Yes
4	Yes	No	Yes
4.5	No	No	No
5	No	No	No
5.5	Yes	No	Yes
6	Yes	No	Yes
6.5	No	No	No
7	No	No	No

Table 6: Interlacing of zeros of $G(z; 3, b)$ and of its derivative

b	Real Parts	Imaginary Parts	Modulus
0	Yes	No	Yes
0.5	Yes	No	Yes
1	Yes	No	Yes
1.5	Yes	No	Yes
2	Yes	No	Yes
2.5	Yes	No	Yes
3	Yes	No	Yes
3.5	Yes	No	Yes
4	Yes	No	Yes
4.5	Yes	No	Yes
5	Yes	No	Yes
5.5	No	No	No
6	Yes	No	Yes
6.5	Yes	No	Yes
7	Yes	No	Yes

Table 7: Interlacing of zeros of $G(z; 3.5, b)$ and of its derivative

b	Real Parts	Imaginary Parts	Modulus
0	Yes	No	Yes
0.5	Yes	No	Yes
1	Yes	No	Yes
1.5	Yes	No	Yes
2	Yes	No	Yes
2.5	Yes	No	Yes
3	Yes	No	Yes
3.5	Yes	No	Yes
4	Yes	No	Yes
4.5	Yes	No	Yes
5	Yes	No	Yes
5.5	Yes	No	Yes
6	No	No	No
6.5	No	No	No
7	Yes	No	Yes

Zeros of $\Phi_1(z) + 0.1\Phi_2(z)$ in rectangle with corners (0.01,0), (250,50).

14.05399773051498293782360,
20.70491329139074401966912+2.616844866452340062733042*I,
26.12337134396348222740848+7.032478148501969546727520*I,
31.55619859716174917719168+10.63967862312023459988132*I,
36.77452448915498753725338+13.67393598760348829399444*I,
41.77978361595260905217632+16.35775960161389517283583*I,
46.60558394536003677261830+18.80225363994308222394823*I,
51.28133970+21.07020087*I,
55.82997811+23.20092762*I,
60.26925938+25.22096602*I,
64.61314132+27.14921718*I,
68.87278790+28.99971130*I,
73.05728437+30.78320189*I,
77.17413840+32.50815184*I,
81.22963952+34.18136412*I,
85.22911935+35.80840254*I,
89.17714710+37.39389060*I,
93.07767478+38.94171735*I,
96.93415065+40.45519570*I,
100.7496044+41.93717241*I,
104.5267156+43.39011464*I,
108.2678706+44.81618052*I,
111.9752060+46.21726886*I,
115.6506419+47.59506093*I,
119.2959142+48.95105541*I

Zeros of $\Phi_1(z) + 0.5\Phi_2(z)$ in rectangle with corners (0.01,0), (250,50).

14.08902220046523054687934,
 21.12619675437600853982743+2.167809862399044817261300*I,
 26.49925561241465900899269+6.518830488201067516712930*I,
 31.86281888297644346624764+10.14336746433991744098012*I,
 37.04061839657234288724122+13.19772765785699083108784*I,
 42.01918363468893300974405+15.89946490084455881257690*I,
 46.82590461178311378509967+18.35899602252905948556528*I,
 51.48714365+20.63964558*I,
 56.02425940+22.78124952*I,
 60.45410138+24.81073198*I,
 64.79006670+26.74728875*I,
 69.04294488+28.60516290*I,
 73.22156696+30.39527466*I,
 77.33325752+32.12621185*I,
 81.38417205+33.80487628*I,
 85.37954140+35.43690962*I,
 89.32385810+37.02700166*I,
 93.22101067+38.57908837*I,
 97.07439923+40.09652760*I,
 100.8870152+41.58220032*I,
 104.6615056+43.03860450*I,
 108.4002298+44.46792244*I,
 112.1053006+45.87207420*I,
 115.7786228+47.25276093*I,
 119.4219142+48.61149393*I,
 123.0367398+49.94963297*I

Zeros of $\Phi_1(z) + 0.9\Phi_2(z)$ in rectangle with corners (0.01,0), (250,50).

14.12540279204329297838269,
 22.06024626629065768582840+.6061840082007214240786940*I,
 27.53884211673404487188027+5.151988671745261134824207*I,
 32.71014677011416973696234+8.808504595278554625647915*I,
 37.77790937484626471097612+11.90936008245477481533350*I,
 42.68217959113845045177974+14.65533585860379427503230*I,
 47.43554640256625947161372+17.15328712711606368308480*I,
 52.05612020+19.46695909*I,
 56.56095710+21.63714420*I,
 60.96437863+23.69163755*I,
 65.27818550+25.65028656*I,
 69.51214950+27.52788542*I,
 73.67436573+29.33574212*I,
 77.77164703+31.08276078*I,
 81.80976600+32.77609674*I,
 85.79368880+34.42160532*I,
 89.72766933+36.02412397*I,
 93.61542830+37.58772657*I,
 97.46023565+39.11587714*I,
 101.2649633+40.61156436*I,
 105.0321707+42.07734953*I,
 108.7641444+43.51548360*I,
 112.4629346+44.92794733*I,
 116.1303883+46.31648341*I,
 119.7681929+47.68266510*I,
 123.3778470+49.02785824*I

Zeros of $\Phi_1(z) + 0.95\Phi_2(z)$ in rectangle with corners (0.01,0), (250,50).

14.13005217571049725343824,
 21.37866821884876502761078,
 23.33324390918326617968587,
 27.99305572733915135628770+4.583648936855093368284408*I,
 33.07772223651098839298118+8.244043941410326529377250*I,
 38.09893096663158918113470+11.36157615057808481353196*I,
 42.97084922671673637220183+14.12444034395922309971465*I,
 47.70082869466270341596556+16.63769086636915403960208*I,
 52.30353035+18.96478334*I,
 56.79417375+21.14672842*I,
 61.18595615+23.21158270*I,
 65.49002785+25.17946198*I,
 69.71566370+27.06532218*I,
 73.87068145+28.88064326*I,
 77.96164925+30.63445708*I,
 81.99416110+32.33399442*I,
 85.97304930+33.98519285*I,
 89.90250925+35.59298711*I,
 93.78615740+37.16148063*I,
 97.62721980+38.69420856*I,
 101.4284894+40.19413687*I,
 105.1925158+41.66391734*I,
 108.9215435+43.10581510*I,
 112.6175914+44.52182683*I,
 116.2824866+45.91372360*I,
 119.9178737+47.28304363*I,
 123.5253008+48.63127754*I,
 127.1060884+49.95961580*I

Zeros of $\Phi_1(z) + 0.1\Phi_3(z)$ in rectangle with corners (0.01,0), (250,50).

14.04543958246877586032484,
20.62534604921236251942571+2.697151806087224635627440*I,
26.05616698613344410640406+7.125359662760955155036280*I,
31.50143143782242948247893+10.72915032137856055739179*I,
36.72702283470204695852392+13.75961404955500621826564*I,
41.73703486879525494792868+16.44012730915123802170981*I,
46.56622874261084814907498+18.88186958225702820877545*I,
51.24456568+21.14750392*I,
55.79525380+23.27625694*I,
60.23621437+25.29458581*I,
64.58150488+27.22133530*I,
68.84235660+29.07049587*I,
73.02789948+30.85279237*I,
77.14567365+32.57666365*I,
81.20199115+34.24889227*I,
85.20220355+35.87503108*I,
89.15089300+37.45969003*I,
93.05202295+39.00675062*I,
96.90904962+40.51951690*I,
100.7250090+42.00082743*I,
104.5025878+43.45314750*I,
108.2441776+44.87862916*I,
111.9519160+46.27916597*I,
115.6277294+47.65643840*I,
119.2733554+49.01193992*I

Zeros of $\Phi_1(z) + 0.5\Phi_3(z)$ in rectangle with corners (0.01,0), (250,50).

14.04543959702460918817180,
20.62534622237496400533206+2.697151661078025645802802*I,
26.05616719635406177579621+7.125359483353992231633490*I,
31.50143167611311917810787+10.72915012267290670561298*I,
36.72702309854009996003425+13.75961382362765780252606*I,
41.73703514999148381619402+16.44012705278297851528629*I,
46.56622903313909943498808+18.88186929612672978282916*I,
51.24456645+21.14750427*I,
55.79525408+23.27625610*I,
60.23621447+25.29458511*I,
64.58150532+27.22133525*I,
68.84235687+29.07049568*I,
73.02789980+30.85279148*I,
77.14567383+32.57666344*I,
81.20199175+34.24889243*I,
85.20220375+35.87503058*I,
89.15089385+37.45968888*I,
93.05202345+39.00675008*I,
96.90904948+40.51951573*I,
100.7250091+42.00082713*I,
104.5025878+43.45314688*I,
108.2441774+44.87862796*I,
111.9519160+46.27916506*I,
115.6277298+47.65643777*I,
119.2733561+49.01193918*I

Zeros of $\Phi_1(z) + 0.9\Phi_3(z)$ in rectangle with corners (0.01,0), (250,50).

14.04543961158044274920602,
 20.62534639553760039288542+2.697151516068796252272386*I,
 26.05616740657474202722894+7.125359303946993756290220*I,
 31.50143191440389805466441+10.72914992396721322430883*I,
 36.72702336237827258427250+13.75961359770025969800936*I,
 41.73703543118786170215194+16.44012679641465257863827*I,
 46.56622932366752495081440+18.88186900999634307062282*I,
 51.24456637+21.14750355*I,
 55.79525415+23.27625600*I,
 60.23621490+25.29458463*I,
 64.58150563+27.22133448*I,
 68.84235734+29.07049534*I,
 73.02789990+30.85279128*I,
 77.14567405+32.57666258*I,
 81.20199196+34.24889172*I,
 85.20220405+35.87503000*I,
 89.15089344+37.45968911*I,
 93.05202360+39.00674944*I,
 96.90905007+40.51951597*I,
 100.7250098+42.00082709*I,
 104.5025886+43.45314706*I,
 108.2441780+44.87862828*I,
 111.9519167+46.27916550*I,
 115.6277294+47.65643691*I,
 119.2733566+49.01193960*I

Zeros of $\Phi_1(z) + 0.95\Phi_3(z)$ in rectangle with corners (0.01,0), (250,50).

14.04543961339992196073126,
20.62534641718293239535228+2.697151497942640440319802*I,
26.05616743285233145895932+7.125359281521116447125940*I,
31.50143194419025168477081+10.72914989912899875269435*I,
36.72702339535805257327973+13.75961356945933144120201*I,
41.73703546633741941571020+16.44012676436860716568103*I,
46.56622935998359039084240+18.88186897423003852396712*I,
51.24456660+21.14750350*I,
55.79525461+23.27625620*I,
60.23621480+25.29458439*I,
64.58150562+27.22133473*I,
68.84235760+29.07049585*I,
73.02790007+30.85279127*I,
77.14567412+32.57666282*I,
81.20199162+34.24889190*I,
85.20220435+35.87503054*I,
89.15089375+37.45968918*I,
93.05202332+39.00674980*I,
96.90905002+40.51951582*I,
100.7250098+42.00082785*I,
104.5025884+43.45314666*I,
108.2441774+44.87862811*I,
111.9519164+46.27916513*I,
115.6277302+47.65643762*I,
119.2733561+49.01193960*I

Zeros of $\Phi_1(z) + 0.1\Phi_2(z) + 0.1\Phi_3(z)$ in rectangle with corners (0.01,0), (250,50).

14.05399773418755034466230,
20.70491333886082893891874+2.616844825965611206674141*I,
26.12337140230047114153132+7.032478098532344406975476*I,
31.55619866324014456746402+10.63967856779154657370195*I,
36.77452456230587970528020+13.67393592474515185310579*I,
41.77978369392041012752898+16.35775953033929013999650*I,
46.60558402592941391873315+18.80225356043522340540990*I,
51.28133956+21.07020050*I,
55.82997844+23.20092714*I,
60.26925967+25.22096656*I,
64.61314128+27.14921788*I,
68.87278797+28.99971094*I,
73.05728466+30.78320188*I,
77.17413933+32.50815283*I,
81.22963957+34.18136395*I,
85.22911905+35.80840212*I,
89.17714735+37.39389068*I,
93.07767473+38.94171703*I,
96.93415150+40.45519616*I,
100.7496048+41.93717310*I,
104.5267162+43.39011519*I,
108.2678707+44.81618044*I,
111.9752060+46.21726793*I,
115.6506417+47.59506047*I,
119.2959150+48.95105538*I

Zeros of $\Phi_1(z) + 0.1\Phi_2(z) + 0.2\Phi_3(z)$ in rectangle with corners (0.01,0), (250,50).

14.05399773786011776639767,
 20.70491338633091650575080+2.616844785478879949760620*I,
 26.12337146063746488382830+7.032478048562716492916476*I,
 31.55619872931854683000773+10.63967851246285545152218*I,
 36.77452463545678108597905+13.67393586188681153874507*I,
 41.77978377188822267575133+16.35775945906467994559670*I,
 46.60558410649880447796098+18.80225348092735774558728*I,
 51.28133960+21.07020026*I,
 55.82997876+23.20092794*I,
 60.26925993+25.22096660*I,
 64.61314153+27.14921761*I,
 68.87278792+28.99971076*I,
 73.05728475+30.78320185*I,
 77.17413892+32.50815204*I,
 81.22963955+34.18136446*I,
 85.22911915+35.80840218*I,
 89.17714645+37.39388984*I,
 93.07767580+38.94171785*I,
 96.93415100+40.45519538*I,
 100.7496049+41.93717285*I,
 104.5267156+43.39011386*I,
 108.2678720+44.81618108*I,
 111.9752066+46.21726845*I,
 115.6506416+47.59506036*I,
 119.2959148+48.95105482*I

Zeros of $\Phi_1(z) + 0.5\Phi_2(z) + 0.5\Phi_3(z)$ in rectangle with corners (0.01,0), (250,50).

14.08902221953875717720683,
 21.12619714704588295877575+2.167809477973057268501037*I,
 26.49925613478898875228767+6.518830031877912285567943*I,
 31.86281947201906223180428+10.14336695979476421029133*I,
 37.04061904813790194146956+13.19772708711597376811564*I,
 42.01918432936108586212063+15.89946425628923812924865*I,
 46.82590533031728749393905+18.35899530555391945673897*I,
 51.48714348+20.63964522*I,
 56.02425935+22.78124805*I,
 60.45410380+24.81073310*I,
 64.79006690+26.74728712*I,
 69.04294573+28.60516210*I,
 73.22156768+30.39527250*I,
 77.33325836+32.12621022*I,
 81.38417333+33.80487597*I,
 85.37954206+35.43690894*I,
 89.32385833+37.02700000*I,
 93.22101060+38.57908714*I,
 97.07440018+40.09652722*I,
 100.8870153+41.58219964*I,
 104.6615063+43.03860408*I,
 108.4002304+44.46792129*I,
 112.1053015+45.87207240*I,
 115.7786245+47.25275960*I,
 119.4219149+48.61149127*I,
 123.0367384+49.94962946*I

Zeros of $\Phi_1(z) + 0.5\Phi_2(z) + 0.95\Phi_3(z)$ in rectangle with corners (0.01,0), (250,50).

14.08902223670493149306462,
 21.12619750044893466129808+2.167809131989472510141997*I,
 26.49925660492621971007712+6.518829621186868656515712*I,
 31.86282000215789149555782+10.14336650570389727970169*I,
 37.04061963454753639489322+13.19772657344877509532047*I,
 42.01918495456680828822414+15.89946367618907836883441*I,
 46.82590597699896111520046+18.35899466027580847880506*I,
 51.48714383+20.63964428*I,
 56.02426005+22.78124754*I,
 60.45410452+24.81073226*I,
 64.79006775+26.74728610*I,
 69.04294553+28.60515840*I,
 73.22156905+30.39527181*I,
 77.33325862+32.12620937*I,
 81.38417380+33.80487441*I,
 85.37954262+35.43690778*I,
 89.32385850+37.02699822*I,
 93.22101193+38.57908773*I,
 97.07440083+40.09652577*I,
 100.8870162+41.58219880*I,
 104.6615065+43.03860300*I,
 108.4002300+44.46791994*I,
 112.1053017+45.87207261*I,
 115.7786230+47.25275740*I,
 119.4219166+48.61149250*I,
 123.0367396+49.94962908*I

Zeros of $\Phi_1(z) + 0.2\Phi_2(z) + 0.1\Phi_3(z)$ in rectangle with corners (0.01,0), (250,50).

```

14.06263333033717458644054,
20.79245368703654469330030+2.527195910558330219737487*I,
26.19856049153492015738472+6.928938817633301664380444*I,
31.61749575438356178149142+10.53984104434132980823528*I,
36.82769852345589411310854+13.57827007370192510589474*I,
41.82763232094792350431597+16.26575860510984539611731*I,
46.64962923168197349770616+18.71330860490054285062478*I,
51.32249140+20.98382859*I,
55.86883300+23.11675257*I,
60.30623280+25.13869802*I,
64.64853565+27.06862288*I,
68.90683255+28.92060356*I,
73.09015730+30.70542638*I,
77.20598096+32.43158124*I,
81.26056585+34.10588858*I,
85.25922540+35.73393233*I,
89.20651190+37.32034470*I,
93.10636653+38.86902857*I,
96.96222630+40.38330328*I,
100.7771131+41.86602160*I,
104.5537007+43.31965893*I,
108.2943705+44.74637766*I,
112.0012532+46.14808096*I,
115.6762668+47.52645439*I,
119.3211446+48.88299783*I

```

Zeros of $\Phi_1(z) + 0.95\Phi_2(z) + 0.5\Phi_3(z)$ in rectangle with corners (0.01,0), (250,50).

14.13005219566626258257954,
 23.33325107313681444452822,
 27.99306090894274240308300+4.583644205971031946122978*I,
 33.07772791106543955947734+8.244038643757668850342223*I,
 38.09893723213515652968370+11.36157025351404924285491*I,
 42.97085591362847867937990+14.12443377629517589131135*I,
 47.70083563459427905780926+16.63768363624691870807804*I,
 52.30353603833716565597965+18.96476767032515570685753*I,
 56.79417383962384497471800+21.14672056553926420560904*I,
 61.18596823966500289600705+23.21158415399288345838686*I,
 65.49004187817750170618910+25.17946403173408972054518*I,
 69.71568633742799937358055+27.06532314476346997682178*I,
 73.87069517299449124771405+28.88064119067159309217414*I,
 77.96165311298997073344600+30.63444727343977736828145*I,
 81.99417044461233775922020+32.33399179022320120021543*I,
 85.97306750296842268334940+33.98519962536481739751872*I,
 89.90251925008387023826190+35.59298546247651246101206*I,
 93.78616884440681810335020+37.16147908097280996417924*I,
 97.62721743840364925692815+38.69419008021822437647760*I,
 101.4284957453640767057470+40.19413076780517174187258*I,
 105.1925215635635328340496+41.66390947600578522762427*I,
 108.9215464082365810451394+43.10580254622254254298910*I,
 112.6175936274722452020543+44.52181064315906899235939*I,
 116.2824898043963691423927+45.91370336925557608471330*I,
 119.9178908224753738153508+47.28305501504296244642328*I,
 123.5253036540498486633952+48.63127350420719084017235*I,
 127.1061046949206939817296+49.95962405063400791183162*I

References

- [BCRW08] P. Borwein, S. Choi, B. Rooney, and A Weirathumuller. The Riemann Hypothesis. CMS Books in Mathematics, Springer, New York, NY, 2008.
- [CS07] M. Chudnovsky and P. Seymour. The roots of the independence polynomial of a claw free graph. *J. Combin. Theory Ser. Bm* 97(3):350-357, 2007.
- [Edw01] H.M. Edwards. Riemann's Zeta Function. Dover Publications Inc., Mineola, NY, 2001.
- [Hag11] J. Haglund. Some conjectures on the zeros of approximates to the Riemann Xi-function and incomplete gamma functions. *Cent. Eur. J. Math.*, 9(2):302-318, 2011.
- [SS03] E.M. Stein and R. Shakarchi. Complex Analysis. Princeton Lectures in Analysis, Princeton University Press, Princeton, NJ, 2003.